FLORIDA STATE UNIVERSITY

COLLEGE OF SOCIAL SCIENCES

EVIDENCE FOR A SOLAR INFLUENCE ON U.S.-AFFECTING

HURRICANES

By

ROBERT EDWARD HODGES

A Thesis submitted to the
Department of Geography
in partial fulfillment of the
requirements for the degree of
Master of Science

Degree Awarded:
Summer Semester, 2009

The members of the committee approve the thesis of Robert Edward Hodges defended on July 2, 2009.

_____

James B. Elsner
Professor Directing Thesis

_____

Thomas H. Jagger
Committee Member

_____

J. Anthony Stallins
Committee Member

_____

L. Jordan
Committee Member

The Graduate School has verified and approved the above-named committee members.

"It is the glory of God to conceal a thing:
    but the honour of kings is to search out a matter."

-Proverbs 25:2 (King James Version)

ACKNOWLEDGEMENTS

TABLE OF CONTENTS

LIST OF TABLES

LIST OF FIGURES

ABSTRACT

This study examines the robustness of the proposed modern solar activity / hurricane frequency relationship in light of recently compiled Atlantic hurricane records made available for the period 1700-1850. Constructing a thermodynamic efficiency for hurricanes utilizing mean monthly sunspot numbers (SSN), a Bayesian model that incorporates HURDAT (1851-2008) and Chenoweth archive (1700-1850) datasets is employed to maximize the information about the sun-hurricane relationship through the centuries. The information contained within the Chenoweth archive adds support to the hypothesis that solar variation influences hurricane activity. Results have impacts for U.S. seasonal hurricane science, as well as life and property for coastal and near-coastal populations.

CHAPTER 1

INTRODUCTION

"Start with 100,000 cubic miles of luxuriant tropical air, juicy with the humidity from a vacationer's dream of summery ocean waters. Stir it with coalescing thunderstorms and a hint of Coriolis force, just enough to shrug that inconceivable tonnage of airy mass into a spin. Keep the wind shear low to tighten the clouds' organization. Let thermodynamics loosen the brakes: The hot air rises, the surface pressure falls, and the spin accelerates. Rain pours down but the clouds inhale fresh water vapor even faster. Now the saturated moving air is a vast heat engine, and what was a sailor's idyll has become a monster consuming the sky, ripping at the sea. Hot, impatient wind racing twice as fast as a freight train obliterates everything in its way."
-- John Rennie, Foreword, <u>Hemingway's Hurricane</u> (Scott 2006)

Motivation for this study comes from an interest to better understand how variations in solar activity might be affecting North Atlantic hurricanes. To explicate the sun-hurricane relationship in this study, a review of integral processes and definitions is required. This section addresses the physical background of hurricane characteristics and solar processes.

Hurricane Characteristics

Tropical cyclones are large storms that are characterized by heavy rain, winds, and extremely low surface pressures, having sustained winds of 33 m/s (74 mph). Originating from tropical latitudes (north of 10° N), these storms can persist for well over 3 weeks as they progress through the Atlantic Ocean basin. Mid-latitude non-tropical cyclones (MLNTC) rely on similar principal atmospheric processes, such as rising air and the resultant energy exchanges from evaporation and condensation. However, MLNTC reliance on strong upper-level winds ("jet streaks") as an outflow mechanism for rising air markedly differentiates them from their tropical cousins. As a result, MLNTC vertical storm structure in a mature cyclone is tilted toward the strong upper-level winds from the surface, where advancing cold air leads at the surface, helping to increase surface lifting of air. Hurricanes, the idealized mature tropical cyclone, feature a different vertical structure. Instead of strong upper level winds and pressures providing

a dynamic outflow for vertical motion, hurricane vertical motion occurs under upper level high pressure, created in response to its own intense continued convection. Convection is one of the primary transfer processes of heat and mass (in the form of water vapor) in a fluid (Incropera & De Witt 1996). The tropical troposphere, the lowest 16 km of Earth's atmosphere separating the troposphere and stratosphere (Brasseur & Solomon 2005), features this violent vertical transport of heat and water vapor, resulting in the release of latent heat from water vapor condensing. When rising air reaches the tropopause, it encounters a layer of air warmer than the rising air and subsides. In this way hurricanes vent the accumulated surface air. The hurricane vertical structure remains orthogonal ("stacked") to the Earth's surface and upper level high.

Hurricanes can fill the entire vertical extent of the tropical troposphere and translate incredible amounts of energy from the ocean to the atmosphere via latent heat released from the condensation of rising ocean-fed moisture. But their development and intensification are highly dependent on ambient influences. Changes in atmospheric water vapor composition, steering currents, sea surface temperatures, or upper-tropospheric temperatures play significant controlling factors toward determining tropical cyclone intensity. In fact, the prediction of hurricane intensity changes is one of the great unsolved problems of tropical meteorology.

Relative humidity of an atmospheric layer can increase or decrease the buoyancy of air rising through it. Dry air entraining into the storm can decrease convection and interrupt the hurricane's efficiency of utilizing the latent heat release from evaporation, inhibiting intensification or even leading to decay. Mean layer winds for 100mb through 1000mb (Dong and Neumann 1986) often provide the mechanism for direction and translational speed of hurricanes and can be produced from semi-permanent (e.g., North Atlantic Oscillation, El Nino Southern Oscillation) or seasonal (e.g., mid-latitude baroclinic cyclones, frontal boundaries) features. If winds are strong enough, shearing can weaken these giant yet fragile storms.

The last two factors, sea-surface temperatures and upper tropospheric temperatures, constitute the concomitant physical processes we will explore in this study. Sea-surface temperatures provide the warm source for the moisture saturation and heating of surface air that can lead to rising air and convection. The latent release of heat from condensation is the primary source of energy for the hurricane. If temperatures are too low, the convective process is inhibited. For this reason North Atlantic hurricane season occurs in hemispheric summer.

Upper tropospheric temperatures are cooler than air temperatures near the surface. Unlike the stratosphere, tropospheric temperature decreases with height, a consequence of reflected terrestrial longwave radiation decreasing as one moves away from the Earth's surface and volumetric expansion of air which results in an energy and, thus, temperature decrease. The temperature at which the atmosphere decreases with height is referred to as the lapse rate (Ackerman & Knox 2003). The buoyancy of a theoretical parcel of rising air is determined by its temperature in relationship to its ambient environmental temperature: If a parcel is warmer than the air layer it is entering into, it will continue to rise. If a parcel is cooler, the parcel subsides. Also, moisture content (saturation) of a parcel affects this buoyancy. A rising saturated parcel will cool more slowly than an unsaturated parcel due to the release of latent heat from condensation partially countering the cooling from volumetric expansion. Atmospheric humidity plays a major role in vertical motion in the troposphere. But ambient temperatures significantly impact air parcel buoyancy.

The thermodynamic (the study of heat / mechanical work transformation (Fermi 1956) implications of cooler upper air temperatures are realized in terms of a thermal efficiency, characterizing the vertical motion process within thunderstorms and, on a larger scale, hurricanes. This theoretical model is a perfectly efficient model of converting energy from heat to kinesis (i.e., thermal energy to mechanical work). However, energy, mostly in the form of heat, is lost at multiple points in the cycle, lowering the efficiency. In this light, Emanuel (1991) argues that only a small amount of energy in the convective process is available for the generation of wind (mechanical) energy, usually on the order 1/3. This implies that 1/3 of all available energy derived from the release of latent heat (into sensible heat) from evaporation actually is represented as a hurricane's wind intensity. The efficiency is characterized by

$$\epsilon = \frac{T_s - T_o}{T_s}$$

where T_s represents temperature of the heat source (i.e., sea-surface temperatures) and T_o represents outflow temperature (Emanuel 1991). The difference between surface and upper-tropospheric temperatures represents a potential energy available for the generation of wind

energy in hurricanes. Maximum potential intensity (hereafter, MPI) theory stipulates that a hurricane's intensity is proportional to the thermodynamic efficiency between input energy (entropy gain from ocean/atmosphere interaction) and outflow venting (mechanical dissipation) (Miller 1958; Emanuel 1991; Holland 1997; Bister and Emanuel 1998), all else being equal.

An increase (decrease) in surface (upper-tropospheric) temperature would increase the thermodynamic potential energy available for convection. Emanuel (1991) estimates that 10^8 Jm^{-2} would be needed to achieve thermodynamic equilibrium (enthalpy) between the surface and lower stratosphere, an enormous amount. As a result, the change in inflow / outflow temperatures of a given tropical system alters its potential energy yield and MPI.

Solar Processes

While hurricane development depends on optimal sea-surface or upper tropospheric temperatures the sun's role in driving the Earth's climate is paramount. Heating of our planet provided by this star constitutes the primary impetus for Earth's atmospheric processes. The uneven distribution of heating of our planet leads to thermodynamic variability and instability. Just as seasons are a hemispheric response to the tilting of the Earth's axis and change in direct sunlight, the sun plays the critical role in determining temperatures, with its short- and long-wave radiation impacting various atmospheric layers.

The sun is the center of the solar system and provides the Earth with heat and light. Almost ¾ of the sun's total mass is hydrogen (Basu et al 2008). Nuclear transformations from hydrogen to helium, deuterium, beryllium, and lithium comprise the sun's continuous fusion cycle called the p-p (proton-proton) chain, where hydrogen fusion (into helium) is responsible for 85% of the sun's energy output (Salpeter 1952).

Sunspots are visible disturbances on the surface of the sun resulting from intense magnetic fields associated with the geographic switching of magnetic poles that occurs, on average, every 11 years known as the solar dynamo, or solar magnetic cycle. Sunspots consist of dark central cores (*umbra*, Latin for "shadow") in various shapes (*penumbra*, Latin for "almost shadow") (Weiss 2007). Their appearance indicates an increasingly magnetically-active sun, often accompanied by increased solar prominences and coronal mass ejections. The sunspot is actually a result of convective inhibition of solar plasma from magnetic fields. Though the

sunspots are cooler (darker) and decrease solar luminosity, cloud-like features just above sunspot clusters called *faculae* are about 300 K hotter (brighter) than normal surface temperatures of 5,777 K (Stanford 2009). The result is higher outgoing Total Solar Irradiance (TSI) and higher ultraviolet (UV) and extreme ultraviolet (EUV) radiation reaching Earth during periods of high sunspots.

TSI is the amount of solar radiative energy impacting the Earth's upper atmosphere and averages 1367 Wm^{-2} (+/- 4 Wm^{-2}). It varies in phase with the solar magnetic activity cycle and, thus, ultraviolet radiation. While variations of approximately .1% TSI can occur within a given 11 year cycle, shortwave UV and EUV intensity is known to vary as much as 10% within a given cycle. The atmospheric impacts of a 10% UV and EUV variation can be significant (Hoyt & Schatten 1997).

Planck's law describes the amount of light emitted (spectral irradiance) in terms of electromagnetic radiation for all wavelengths for a given temperature (Rybicki 1979). With the sun's surface temperature of 5,777 K, electromagnetic radiation is emitted most abundantly in the visible spectrum (380 nm – 760 nm), followed by the ultraviolet (UV) spectrum (10 nm – 400 nm). UV radiation is categorized into 3 bands: UV-A (400 nm – 320 nm), UV-B (320 nm – 280 nm), and UV-C (280 nm – 200 nm) (Ghosh 2002). Absorption of these UV rays is the realm of ozone and ozone production. Ozone absorbs UV most abundantly at wavelengths of 200 nm – 310 nm range, known as the Hartley band (Assembly 1977). The Mg II index (Heath and Schlesinger, 1986; Viereck and Puga, 1999) measures solar UV variations, beginning in 1991, at wavelengths near 200 nm, a critical ozone production wavelength. Hood (2003) utilized this index to find that the tropical tropopause temperatures responded to increased UV radiation. Increases in upper-tropospheric temperature corresponded strongly with solar activity maximums (Pap & Fox 2004), agreeing with the findings from NCEP/NCAR stratospheric temperature reanalyses (Labitzke 2002). Thusly, upper tropospheric warming occurs during periods of high solar activity due to increased UV radiation ozone absorption.

Higher solar activity has also been linked with increased global SST. Upper ocean temperatures were shown to increase during periods of increased solar activity over most of the tropical oceans (White et al., 1997, 1998). Warming at the surface increases hurricane MPI, per the description in the previous section. Conversely, warming aloft caps potential available energy and hurricane intensification. The bicameral effect from increased sunspots through warmer sea

surface temperatures (hereafter, SST) and warmer upper tropospheric temperatures (hereafter, UTT) prevents a univariate approach toward describing the actual solar influence on hurricanes.

The idea for a solar influence impact upon hurricanes was first discovered in 1872, which found that Indian Ocean hurricane frequency increased when sunspots increased (Meldrum 1872). The study was ported to the North Atlantic (Poey 1873). Unfortunately, information about the relationship was not available, but a relationship was found. Elsner & Jagger (2008) continue the sun-hurricane relationship investigation in the North Atlantic. Western Caribbean in-season SSTs are nearly always warm enough for hurricane formation, while eastern Caribbean and tropical Atlantic SST are generally lower and much more spatially confined. With MPI optimal temperatures of 26 – 28 °C (Holland 1997) seasonally in place for the western Caribbean, a controlled spatial domain exists for examining a counter thermodynamic factor (UTT) to SST. Utilizing a Poisson generalized linear model (GLM) and accounting for shear and steering currents, the western (eastern) basin demonstrated a significant negative (positive) relationship between solar activity and hurricane frequency, corroborating the thermodynamic inflow/outflow temperature argument. The relationship was shown to be statistically significant after controlling for other factors known to affect hurricane frequency.

For the purpose of our study, we are interested in hurricane counts as our dependent variable. Intensity and hurricane counts (frequency) are not mutually independent characteristics (Elsner & Jagger 2008). A closed system becomes a tropical storm once sustained winds reach 17 m/s. Likewise, the system then becomes a hurricane once sustained winds reach 33 m/s. All else being equal, as hurricane season[1] characteristics (e.g., sea-surface temperatures, upper air temperatures, semi-permanent synoptic scale features, etc.) alter MPI we expect hurricane frequencies to respond accordingly.

Hypothesis and Objective

The sun-hurricane relationship was demonstrated in Elsner & Jagger (2008) as significantly suppressing hurricane activity during periods of high SSN for regions of sufficient

---

[1] The North Atlantic hurricane season is temporally defined from 1 June through 30 November. 97% of all tropical cyclone activity has occurred between these dates since 1856 (http://www.aoml.noaa.gov/hrd/tcfaq/tcfaqHED.html).

SST. We aim to build off of this research and hypothesize that sun-hurricane relationship can be more precisely defined through the use of extended hurricane records (Chenoweth 2006). This study will examine the robustness of the sun-hurricane relationship in light of recently compiled hurricane observations prior to modern data (Chenoweth 2006).

First, the relationship will be re-examined within the modern (1851-2008) HURDAT dataset, and a seasonal model will be utilized to explicate the impact of SSN, along with SST and temporal constraints, upon U.S.-landfalling hurricane frequency counts. Then, SSN will be used as a sole data source for examining the sun-hurricane relationship, with the construction of a thermodynamic efficiency from peripheral and core month SSN to be tested in a seasonal model. Ultimately, a Bayesian model that makes use of additional U.S.-landfalling hurricane counts back to 1749 will be constructed to maximize the information about the sun-hurricane relationship across the centuries.

Chapter 2 will elaborate upon the nature of the dependent variable (hurricane records) and independent variables (sunspot numbers and sea-surface temperatures) used in our study. Chapter 3 will examine the sun-hurricane relationship with respect to modern data records, and provide a thermodynamic method toward this discovery. Chapter 4 will extend this method to records prior to those examined in Chapter 3, utilizing historical hurricane records from Chenoweth (2006) and SSN data (National Geophysical Data Center 2009), to be followed by a summary and conclusions.

CHAPTER 2

DATA

This study incorporates modern and historical hurricane records, sea surface temperatures (SST), and monthly mean group sunspot numbers (SSN) toward testing the robustness of the sun-hurricane relationship. This chapter looks at a description of modern hurricane records, with an inclusion of a new compendium of hurricane observations prior to modern records. Finally, SST and SSN data are outlined.

Hurricane Records

The National Hurricane Center (NHC) houses the North Atlantic-basin hurricane database (HURDAT, or Best Track), containing dates, tracks, wind speeds, and central pressure values as available, providing the best available modern hurricane information dating back to 1851 (Jarvinen et al. 1984). Tropical tempestologists rely heavily, if not exclusively, on this record for performing quantitative analyses, producing research such as hurricane return levels (Elsner et al 2008); risk analysis using hurricane destructiveness power predictions (Bogen et al 2007); and predictive modeling for storm seasons (Larow 2008). With refining work begun by the late Jose Fernandez-Partagás (Partagás & Diaz 1996), over 5000 additions and alterations have been approved by the NHC Best Track Change Committee in an effort to improve the accuracy of storm data between 1851-1910 (AOML 2008). The April 2008 version identifies 1,362 unique North Atlantic storms (> 18 m/s) and 819 hurricanes (> 33 m/s), 283 of which affected the U.S. mainland (National Hurricane Center 2008).

Chenoweth's cross-referenced archival of premodern (1700-1850) North Atlantic hurricanes should be of particular interest to North Atlantic storm studies. His work improves upon previous compilations (Poey 1855, Redfield 1863, Tannehill 1938, Ludlum 1963) and provides individual storm positions and dates preceding those listed in the HURDAT compendium. Verifying storm position and dates, Chenoweth conducted a re-analysis of

Ludlum's 1963 work, cross-referencing and validating individual entries using newspaper accounts, weather diaries, and ships' logbooks. Chenoweth's compilation identifies 383 unique storms and 289 hurricanes, 127 of which affected the U.S. mainland (Chenoweth 2006).

For both HURDAT and Chenoweth archive datasets, hurricanes were manually identified as either affecting the US mainland or not based on available information and then counted. All modern record references to U.S. hurricanes refer to those that made U.S. landfall. For the Chenoweth archive, hurricanes listing a U.S. mainland state or region qualified as U.S.-affecting. Chenoweth's archive was digitized for use as a database of individual storm locations (Table 2.1). Individual storm methodology is explicated in Scheitlin et al. (2009). Annual counts of these storms serve as the dependent variable for our statistical modeling, which was accomplished using R (R Development Core Team 2006).

Table 2.1 - A digitized portion of the Chenoweth (2006) archive. Individual event locations are represented for a given storm event. "Track" represents verbatim listings from the archive, which are split into respective observation "Locations" and digitized with appropriate latitude / longitude coordinates.

Year	Month	Fsn	Int	Track	Location	Latitude	Longitude
1700	9	1	HU	South Carolina and Virginia	South Carolina	32.87	-79.63
1700	9	1	HU	South Carolina and Virginia	Virginia	37.29	-75.58
1700	9	2	HU	Barbados	Barbados	13.18	-59.56
1702	9	3	HU	Barbados to 1711N 6949W	Barbados	13.18	-59.56
1702	9	3	HU	Barbados to 1711N 6949W	1711N 6949W	17.18	-69.82
1703	10	4	HU	Virginia to New England	Virginia	37.29	-75.58
1703	10	4	HU	Virginia to New England	New England	42.8	-70.66

Issues of accuracy are inherent in historical observations due to lack of observational density, both temporal and spatial. Table 2.2 outlines the major advances in tropical cyclone observation. Historical documents (personal diaries, newspaper accounts, ships' logbooks) constitute a large segment of paleotempestological data. Geological proxies, such as tree rings, pollen, oxygen isotopes from ocean and ice cores, can also be included toward efforts in reconstructing storm histories that have escaped the reach of an era's technological and observational prowess.

Differences in storm counts between the modern (HURDAT) and prior (Chenoweth archive) storm records may be explained by changes in tropical climatology and/or due to limited opportunities of observation. Given the nature of the collection of premodern observations, knowledge of storm location and occurrence was a function of shipping traffic path frequency

and meteorologically-attuned populations. As such, we assume that storm counts are underrepresented in the Chenoweth archive. An attempt at representing this undercount will be documented in Chapter 4.

Table 2.2 - Advances in tropical cyclone observation (Jarvinen 1984).

Pre-1871	Land observations and Ship logs
1871	Government establishment of Hurricane Warning Service
1905	Ship observations via wireless telegraph
1914	Opening of Panama Canal - shipping boon in tropical Atlantic (Caribbean, Gulf of Mexico)
1918	End of World War I
1937	Radiosonde (weather balloon) network
1944	Organized reconnaissance
1945	End of World War II
1955	Coastal Radar network
1960	Orbiting Sun-synchronous satellites (Visible and Infrared)
1966	Geostationary satellites (Visible only)
1973	Ocean data buoys
1974	Geostationary satellites (Visible and Infrared)
1978	Aircraft-satellite data link
1992	Automated Surface Observing System (ASOS) network[2]
Mid-1990s	Mobile Radar and Observation platforms[3,4]
2005	Aerosonde (unmanned aerial vehicle)[5]

Sea Surface Temperatures

The SST Anomalies data is provided and maintained by the Physical Sciences Division of the Earth System Research Laboratory, NOAA, and is derived from the Kaplan SST dataset (Kaplan et al. 1998). Though observations were sometimes sparse, interpolated SST are available back to 1856 and are recorded monthly and globally by a 5° x 5° lat/long bounding. Utilizing ship observations located in the U.K. Met Office database (Parker et al. 1994), Kaplan's dataset is an analysis which uses optimal estimation from 80 empirical orthogonal functions (EOFs). EOFs are useful for accounting for time-series and spatial patterns.

---

[2] ASOS User's Guide (1998)
[3] TTHRT (Texas Tech Hurricane Research Team, Texas Tech University)
[4] \FCMP (Florida Coastal Monitoring Program)
[5] Aerosonde (2006)

A SST time-series (Figure 2.1) demonstrates the upward-trending SST. For this study unsmoothed monthly mean North Atlantic SST Anomalies (1856-2008) are utilized (Enfield et. al 2001); references in this study to SST imply use of this data set. The methodology (Earth 2009) begins with the 5° X 5° gridded Kaplan SST dataset. An areal weighted average is calculated over the North Atlantic from 0° to 70° N. The results are linearly detrended in an effort to account for climate change affecting the data (Mann & Emanuel 2006). A 121-month smoother can be applied, but for the purpose of this study is not.

Table 2.3 lists seasons corresponding to cool, neutral, and warm SST anomaly years within the extent of the dataset. Demonstrating the importance of the detrended dataset, a value of 22.8°C can correspond with a cool, neutral, or warm phase depending on the sampling year. Warm and cool phase anomaly years will be used, specifically, in the next chapter.
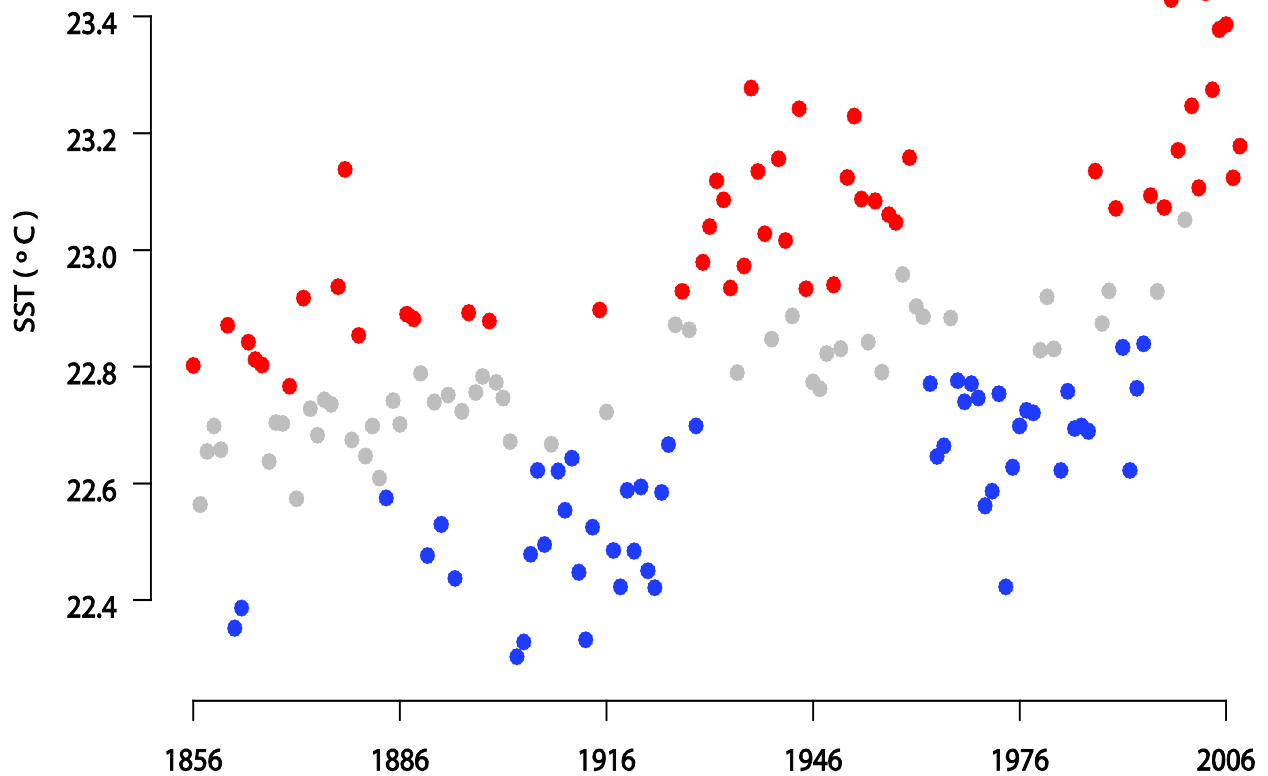
Figure 2.1 - Annual North Atlantic SST from 1851-2008. Blue, gray, and red dots correspond with below, normal, and above-average terciles of AMO anomaly years.

Table 2.3 – Cool (C), Neutral (N), and Warm (W) SST anomaly years for 1856 - 2008. Y denotes the last digit of the year.

Y	185	186	187	188	189	190	191	192	193	194	195	196	197	198	199	200
0	.	N	W	W	C	N	C	C	W	N	N	W	C	N	W	N
1	.	W	N	N	N	N	C	C	W	W	W	N	C	N	C	W
2	.	C	W	N	C	N	C	C	W	W	W	N	C	C	C	W
3	.	C	N	N	N	C	C	C	W	N	W	C	C	C	C	W
4	.	W	N	C	C	C	C	C	W	W	N	C	C	C	C	W
5	.	W	N	N	N	C	W	C	N	W	W	C	C	C	W	W
6	W	N	N	N	W	C	N	N	W	N	N	N	C	C	N	W
7	N	N	W	W	N	C	C	W	W	N	W	C	C	W	W	W
8	N	N	W	W	N	N	C	N	W	N	W	C	C	N	W	W
9	N	N	N	N	W	C	C	C	W	W	N	C	N	N	W	.

Sunspot Numbers

Monthly mean sunspot numbers (SSN) for this study were the International sunspot number as made available by the National Geographic Data Center (National Geophysical Data Center 2009), which was originally constructed by Solar Influences Data Analysis Center, World Data Center at the Royal Observatory of Belgium (Van Der Linden 2009). Reliable monthly observations extend back to 1749. Swiss astronomer Johann Rudolph Wolf introduced a daily measurement technique that observes both total spots observed and the quantity of their clusterings. The data set addresses observed error by incorporating a weighted average of cooperating observations.

Figure 2.2 displays a time-series of (a) U.S.-affecting seasonal hurricanes, (b) SST anomalies, and (c) monthly mean sunspots for the period 1856-2008. U.S.-affecting hurricane counts (~1.78 / season) show no significant trending during the time period; a line of least squares regression yields a slope = -0.001, but at inconclusive statistical significance (P = 0.631). SST anomalies account for time autocorrelation per the section description. The time period reflects almost 14 full solar cycles (Kane 2002, 2009).
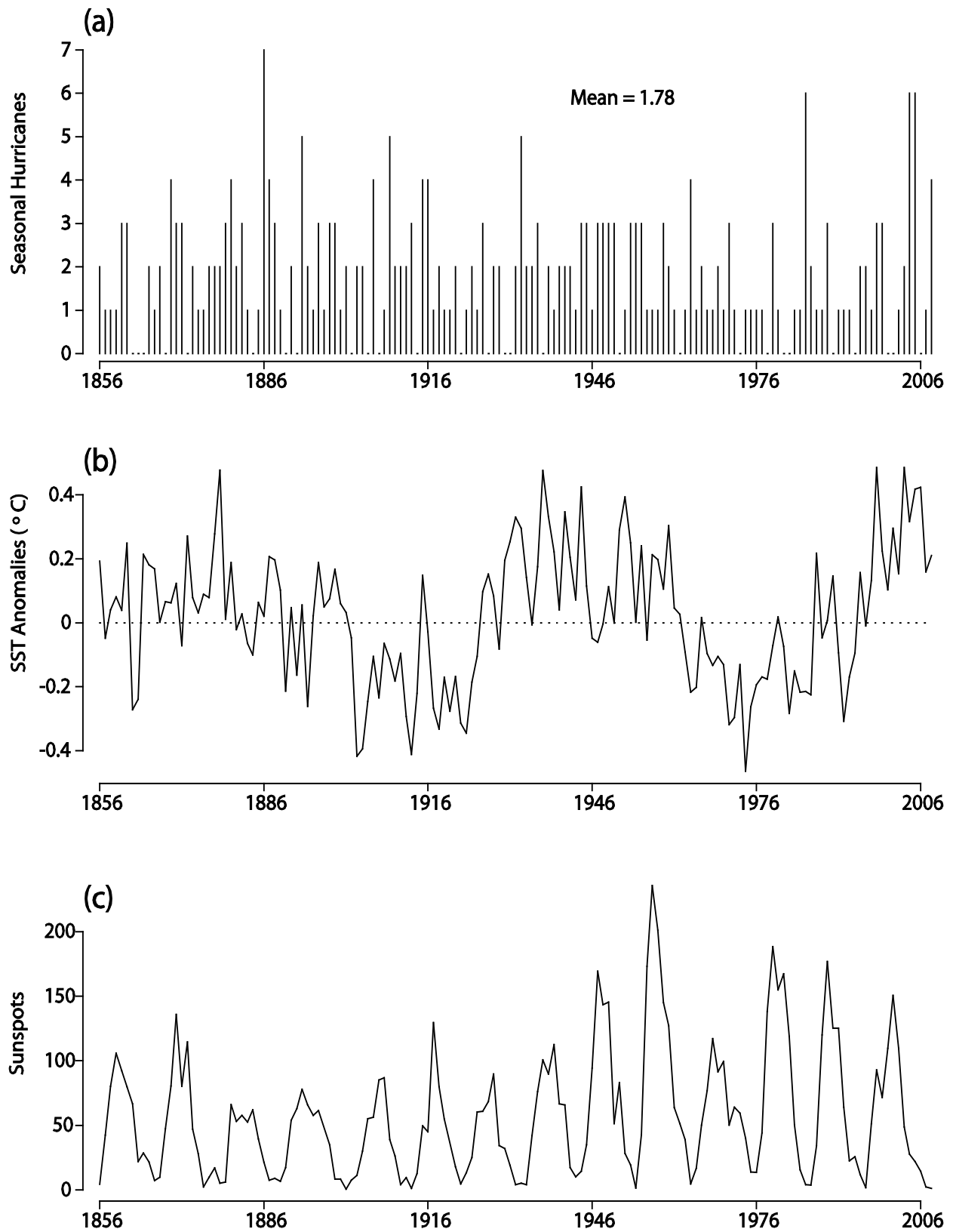
Figure 2.2 - Time series of (a) U.S. seasonal hurricanes, (b) SST anomalies, and (c) monthly mean sunspots for the period 1856-2008.

CHAPTER 3

EVIDENCE FOR A SOLAR INFLUENCE USING MODERN
RECORDS

In their study, Elsner and Jagger (2008) show a geographic difference in the sun-hurricane relationship. Over the Western Atlantic where oceanic heat content is largest, the relationship demonstrates a significant decrease in hurricane frequency for increased sunspots. In contrast, the Eastern Atlantic indicates an increase in hurricane frequency. The Western Atlantic was theorized as demonstrating a thermodynamic inhibition due to warmed upper tropospheric temperatures from increased UV radiation during times of high sunspots. The Eastern Atlantic findings suggest increased SST as overpowering upper level warming during times of high sunspots.

In an exploration similar to their spatial examining of SSN and hurricane frequency, we attempt to create a controlled temporal domain toward eliciting further information about the sun-hurricane relationship. Our use of the word controlled is not meant to imply a change in experimental conditions, as it normally entails; physical geographic events and subsequent observations represent singular opportunities in capturing information. Rather, it refers to a methodological approach toward identifying and approximating the magnitude of covariates (SSN, SST) within this multivariate analysis. Before conducting our statistical investigation, however, we justify our parametric modeling techniques regarding the use of hurricane count information.

The Poisson Nature of Hurricane Counts

Parametric modeling in this study are based on Poisson parameterized distributions, the long held approach to hurricanes as a stochastic event (Smiley 1959), as an approximation for the density of probable outcomes. The usage of the Poisson parameterization requires the event obey the principles characterized by a Poisson process. A Poisson process is predicated on two conditions: 1) As the sampling time interval decreases, event occurrences must not exceed a one

occurrence threshold (a non-temporal concurrence clause); 2) there can be no relationship between count occurrences at any time interval (Elsner & Kara 1999).

Hurricane counts can be considered a quasi-Poisson process. Given that hurricanes can form anywhere within the North Atlantic tropical cyclone source region as well as at any time within a given hurricane season, it is not impossible for concurrent cyclogenesis, though highly unlikely. Also, non-interdependence of events cannot be guaranteed: Hurricane activity can be squelched within a given season, for instance, if a second storm were to traverse the same region as a previous storm ($<$ 2 weeks) by inducing colder-water upwelling and, thus, cooler sea surface temperatures. The cooler sea surface temperatures can weaken and even cause the demise of the following tropical cyclone.

A chief characteristic of the Poisson process approximation relies on the rareness of the measured event. A physical occurrence, such as hurricanes, constitutes a binary count dependent on the threshold of maximum sustained winds of 33 ms^{-1}; a negative hurricane occurrence is a physical and mathematical impossibility. For Poisson distributions, the mean and variance are equal for rare event count data. As counts systemically increase, the distribution will take on a more normally distributed probability density function, characterized by independent mean and variance.

Sun-hurricane Relationship in Modern Data

Assuming a Poisson distribution to model U.S.-affecting hurricane counts, Figure 3.1 reveals that increased September SSN, representing the climatological peak of the North Atlantic hurricane season, results in the decrease in mean U.S.-affecting hurricane frequency. We argue that high September SSN should demonstrate most clearly a suppression of U.S.-affecting hurricane frequency due to warmed UTT.

Figure 3.1a shows the probability distribution of U.S.-affecting hurricanes conditioned on values of September SSN for seasons of above-normal SST. Above-normal SST are described in Chapter 2; specifically, Figure 2.2. For each hurricane count the percent represents the probability of that many hurricanes. For the lowest-tercile September SSN (less than 10 recorded), the probability of zero U.S.-affecting hurricanes occurring is 9%. This probability increases to 20% for highest-tercile September SSN. Conversely, the probability for exactly
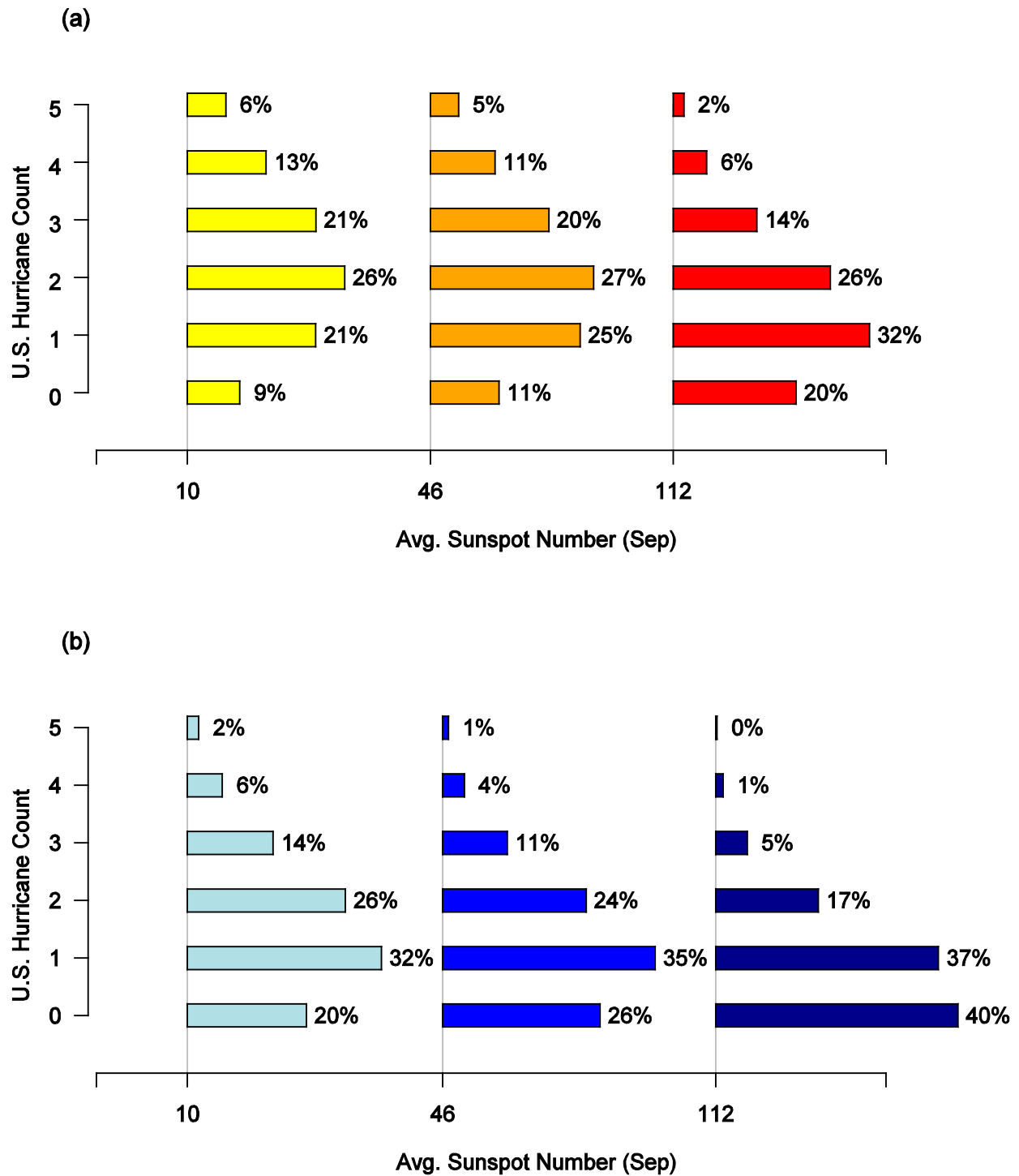
Figure 3.1 - Probability distribution (Poisson) of U.S.-affecting hurricane counts conditional on terciled September sunspot numbers for years of (a) upper- and (b) lower-tercile core-season (August – October) Atlantic Ocean temperature anomalies. Average September sunspots are displayed as the means of their respective terciles. Data spans from 1856 – 2008.

4 hurricanes is 13% and 6% for lowest and highest September SSN, respectively. Likewise, the probability of 3 or more hurricanes occurring dwindles from 40% to 22%. Note that the shape of the distribution is much more symmetric for lowest-tercile SSN.

The second graph (Figure 3.1b) shows the probability distribution conditional on values of September SSN for seasons of below-normal SST. For the lowest-tercile September SSN, the probability of U.S.-affecting hurricanes occurring is 20%. This probability increases to 40% for highest-tercile September SSN. Conversely, the probability for exactly 4 hurricanes is 6% and 1% for lowest and highest September SSN, respectively. Likewise, the probability of 3 or more hurricanes dwindles from 22% to 6%. Also, as mean storm counts decrease with increasing tercile SSN, the distribution takes on an even more skewed distribution.

With hurricane intensity heavily dependent on SST (e.g., Emanuel 1991, Holland 1997, Henderson-Sellers et al 1998), the decrease in overall U.S.-affecting hurricane probabilities of warm SST to cold SST is expected. However, increasing sunspot numbers under both scenarios decrease, demonstrating the effect of warmed upper tropospheric temperatures as an inhibiting thermodynamic factor in hurricane intensity and, thus, frequency.

The correlation between September SSN and U.S.-affecting hurricane counts is modulated by SST. This can be seen in Figure 3.2. The correlation (Pearson) over all years is -0.14 as indicated by the left-most point. The correlation is based on a sample size of N=153 years. Each storm season is considered independent, and the standard error on this correlation estimate is 0.156, providing a 90% confidence interval of (-0.279 , -0.01). The confidence interval is shown in the gray shading. The next point on the graph to the immediate right is the correlation between hurricane counts and SSN after removing the coldest 20% (20th percentile) seasons. The 20th percentile SST value constitutes an anomaly of -0.17°C. The correlation changes negligibly, but with reduced sample size the confidence band widens. The plot shows that the correlation does not change much for the coldest 50% of seasons. However, when 60% of the coldest seasons are removed, the correlation decreases to -0.23 with a 90% confidence interval of (-0.435, -0.035), based on a sample size of 61 years. The correlation continues to decrease as only the warmest years remain. With sample size decreasing accordingly the confidence bands expand, but the relationship between U.S.-affecting hurricane counts and September SSN is statistically significant. The negatively strengthening correlation suggests that the warmest core-season SSTs display the strongest suppressive effects from high September

SSN. Warmer core-season SSTs provide a fertile developing ground for tropical development. As such, suppressed tropical development (i.e., U.S.-landfalling hurricanes) from high September SSN should be most evident then.
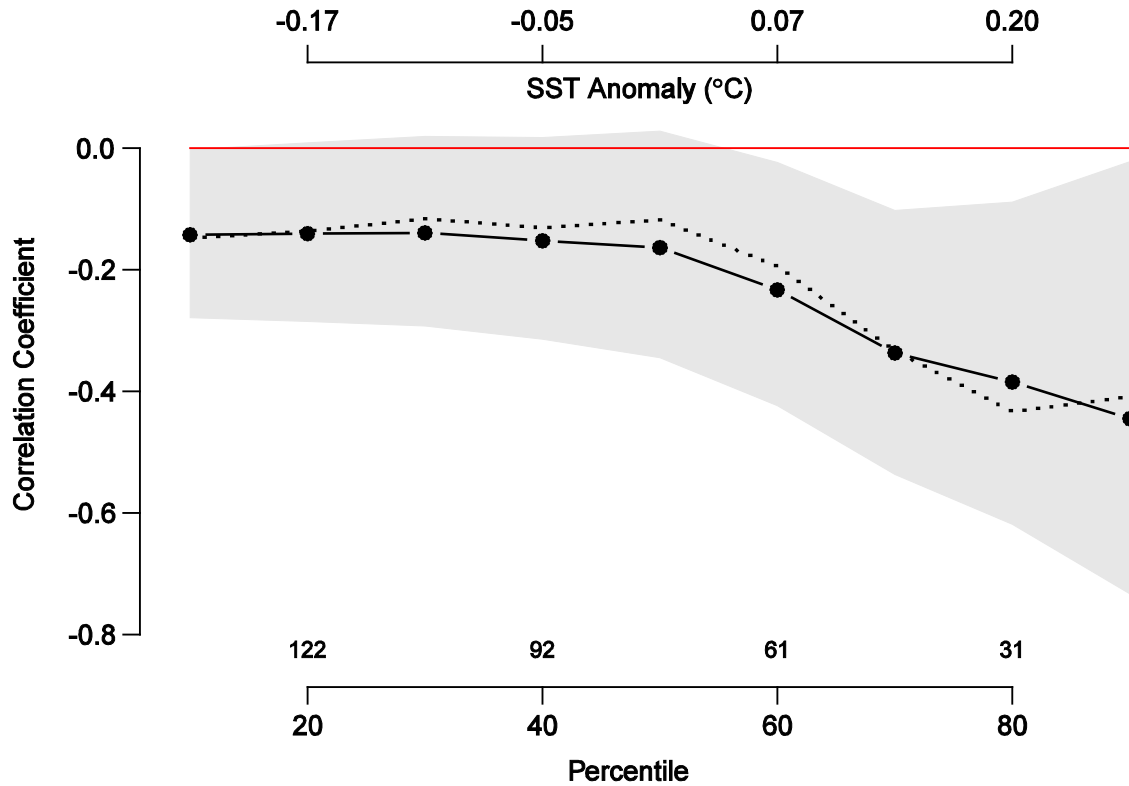
Figure 3.2 – Pearson product-moment (points) and Spearman rank (dashed line) Correlation coefficients between September SSN and U.S.-affecting hurricane counts. The correlations are computed at increasing deciles of August through October averaged SST for the modern period 1856-2008. The shaded region represents the 90% confidence bound at each computed value (Pearson). The number of qualifying seasons are shown above the abscissa.

Bivariate exploration of SSN and SST data (Figures 3.1 and 3.2) has revealed corroborating evidence toward the sun-hurricane relationship in the North Atlantic basin; specifically, that increased SSN and warmer UTT (from increased UV radiation) suppresses U.S.-affecting hurricane frequency. Next we will examine the same datasets, temporally partitioned, in single and multi-variate generalized linear models toward demonstrating their concomitant effects.

Seasonal Model for U.S.-affecting Hurricanes using SSN and SST for 1851-2008

Prior analysis showed that the relationship between SSN and U.S.-affecting hurricanes is also contingent upon on oceanic warmth. This makes physical sense. Hurricanes, as previously described, require the tropical ocean as a continual source of moisture and heat. A baseline of 26.5°C has been the long held minimum for tropical development (e.g., Palmen 1948; Gray 1968, Anthes 1982). Seasons of higher overall SST, all else being equal, should provide a more conducive environment for tropical development. Our previous result indicates the suppressive effect of higher September SSN upon U.S.-affecting hurricane counts, especially during warmer SST hurricane seasons. The more conducive SST seasons, as a result, provide a larger sampling (from increased frequency), which demonstrate a magnitude increase in the negative effects from increased sunspots and UTT warming.

We proceed next by developing a seasonal generalized linear model comprised of September SSN and August through October averaged SST as covariates within a seasonal model of U.S.-affecting hurricane counts in the modern record. Since there is more than one explanatory variable (SST and SSN) it is more useful to use a generalized linear regression model rather than bivariate correlation.

Generalized linear models (hereafter, GLM) are comprised of three elements: A distribution function, a linear predictor, and a canonical link function. Each GLM described herein uses the logarithm of the independent variable (i.e., U.S.-affecting hurricane counts) as the canonical link function to a linear regression of the covariates (i.e., core/peripheral month SSN, AMO). The anti-log of the linear predictor (with other covariates held constant) will produce a factor change in the dependent variable.

The covariate estimate represents the change in the logarithm of the dependent variable (i.e., U.S.-affecting hurricanes) while the other covariates are held constant. Each covariate reduces the degrees of freedom of the model by 1. The significance of the covariate to the model is based on the amount by which the residual deviance decreases with its inclusion in the model. Under the null hypothesis that a covariate is unimportant to the model, the residual deviance has a χ^2 distribution with 1 degree of freedom. A P-value less than 0.05 indicates that the covariate is statistically important to the model after accounting for the variables already present in the

model. Covariates are added to the model sequentially from top to bottom as listed in all tables. Null refers to a model containing no covariates.

Table 3.1 – Coefficients and Analysis of Deviance of a Poisson Regression Model for U.S.-affecting hurricanes (1851-2008) using mean August-October SST ($SST_{Aug-Oct}$) and September SSN (SSN_{Sep}).

Term	Estimate	Degrees of Freedom	Deviance	Residual Degrees of Freedom	Residual Deviance	P-value
NULL	+ 0.695			152	194.207	
$SST_{Aug-Oct}$	+ 0.733	1	6.134	151	188.073	0.013
SSN_{Sep}	- 0.003	1	4.094	150	183.980	0.043

Signs of the parameter estimates (Table 3.1) indicate a contrasting relationship between the covariates: Warm core-season SST increases the probability of a U.S.-affecting hurricane, whereas increasing September SSN decreases the probability of a U.S.-affecting hurricane. The findings are statistically significant and consistent with supporting hurricane theory and the sun-hurricane relationship.

Quantitatively, the model covariate estimates represent the logarithmic response within the dependent variable (i.e., U.S.-affecting hurricane counts) for a one unit covariate increase (with all other covariates held constant). We take the anti-log of the estimate, multiplied by the unit covariate, to find the rate ratio impact upon the dependant variable. Given that interannual SST anomalies vary from (-0.465 °C, +0.485 °C), we interpret the model that an increase of 0.37 °C (95th percentile) in core-season SST increases the probability of a hurricane occurrence by a factor of 1.31 ($e^{+0.73*0.37}$) when September SSN are held constant. August through October averaged SST anomaly increase of 0.48 °C (99th percentile) increases the probability of a hurricane occurrence by a factor of 1.42 ($e^{+0.73*0.48}$).

Conversely, when core-season SST is held constant, a 1 unit increase in September SSN decreases the probability of a hurricane occurrence by a factor of 1.003... ($e^{-0.0026}$). A September SSN value of 145 (95th percentile) decreases the probability of a hurricane occurrence by a factor of 1.46 ($1 / e^{-0.026*145}$). A September SSN value of 193.9 (99th percentile) decreases the probability of a hurricane occurrence by a factor of 1.66 ($1 / e^{-0.0026*193.9}$). $SST_{Aug-Oct}$ demonstrates a greater reduction in deviance than does SSN_{Sep} (6.134, 4.093), indicating that the

model is impacted more heavily by SST. Both terms, though, are statistically significant, reinforcing the previous section's bivariate analysis results that SST and SSN have a pronounced effect upon the frequency of U.S.-affecting hurricanes.

Table 3.2 – Coefficients and Analysis of Deviance of a Poisson Regression Model for U.S.-affecting hurricanes (1851-2008) using September SSN (SSN$_{Sep}$).

Term	Estimate	Degrees of Freedom	Deviance	Residual Degrees of Freedom	Residual Deviance	P-value
NULL	+0.713			157	196.421	
SSN$_{Sep}$	- 0.002	1	3.626	156	192.796	0.063

For both variables listed (Table 3.1), the reduction in residual deviance demonstrates the model "improvement" toward characterizing the relationship of the independent variables upon the (logarithm of) dependent variable. But is the covariate SSN$_{Sep}$ a significant predictor alone toward determining U.S.-affecting hurricane frequency? A Poisson regression of modern data utilizing September SSN as the sole predictor of U.S.-affecting hurricane frequency (Table 3.2) yields the expected negative sign of the coefficient (-0.002) , continuing to demonstrate the suppressive effect of warmed UTT, though at marginal statistical significance (P = 0.063). The removal of the SST component weakens the model, which makes physical sense: SST is a critical component toward hurricane development and thermodynamic evaluation. Therefore, we will continue to investigate the sun-hurricane relationship with respect to SST.

We have previously demonstrated within the modern data (1851-2008) the bicameral effects of September SSN and August through October SST upon U.S.-affecting hurricane counts. Next, we examine the effects of core (September) and peripheral (May, June, July, and November) month SSN as covariates upon U.S.-affecting hurricane frequency. The temporal partitioning will be used to test the sun-hurricane relationship and describe a unique method toward demonstrating a proxy for SST.

Table 3.3 represents GLM parameter estimates and analysis of deviance for a Poisson regression model. Core-season SSN demonstrates a negative coefficient as produced previously, indicating U.S.-affecting hurricane suppression for increased SSN. However, a positive

Table 3.3 – Coefficients and Analysis of Deviance of a Poisson Regression Model for U.S.-affecting hurricanes (1851-2008) using September SSN (SSN$_{Sep}$) and mean May, June, July, and November SSN (SSN$_{May, Jun, Jul, Nov}$).

Term	Estimate	Degrees of Freedom	Deviance	Residual Degrees of Freedom	Residual Deviance	P-value
NULL	+0.654			157	196.421	
SSN$_{Sep}$	- 0.010	1	3.626	156	192.796	0.057
SSN$_{May, Jun, Jul, Nov}$	+0.008	1	4.417	155	188.379	0.036

coefficient is indicated for peripheral month SSN. We propose that this covariate (SSNMay,Jun,Jul,Nov) within the regression model constitutes a SST proxy, where increased SSN over these months results in overall warmer seasonal SST, supporting increased U.S.-affecting hurricanes. Deviance results state that peripheral month SSN carries greater weight toward impacting U.S.-affecting hurricane counts than core month SSN. This result is similar to that obtained in the SSN-SST regression model. Increases in SSNSep for both models result in a decrease in U.S.-affecting hurricanes; SST$_{Aug-Oct}$ and SSN$_{May, Jun, Jul, Nov}$ result in an increase.

However, our approach must take into account potential multicollinearity. Intraseasonal SSN are highly correlated (0.936), given the sinusoidal nature of the solar cycle: A high value in one month implies that its surrounding months will also be high. Collinear variables within a regression model artificially inflate respective standard errors as well as P-values, leading to possible failure in rejecting the null hypothesis (Allison 1999).

SSN Thermodynamic Efficiencies

One method toward mitigating the negative effects of multitcollinearity within a statistical model is by combining the two quasi-independent variables. We have chosen to represent the peak and non-peak months as a single covariate. SSNε within a Poisson GLM (Table 3.4) represents the difference between peripheral and core month SSN as a single covariate, a thermodynamic efficiency between SST and UTT. The model estimate is positive (statistically significant), indicating that higher (lower) efficiencies correspond with higher (lower) U.S.-affecting hurricane frequency.

Referring to the structure outlined in Chapter 1, hurricanes can be thought of as heat engines. Warm moist air is rises from the surface, cools adiabatically, and releases latent heat into the atmosphere. A portion of this energy is used toward wind generation (Emanuel 1991) which becomes one of the observable intensity indicators for hurricanes. The moist warm air continues to rise until matching the temperature of its surroundings. The resultant outflow vents opposite (clockwise) to the rotation of the hurricane (counter-clockwise). To this end, the ambient temperatures at the inflow and outflow determine how much energy is available for use in the hurricane. As such, $SSN_{May, Jun, Jul, Nov}$ and SSN_{Sep} represent a proxy SST-UTT / inflow-outflow temperature modification and, when combined, constitute an efficiency suitable for examining the thermodynamic environment for a given storm season.

The range of efficiencies stretch from -51.7 to + 51.2. As described on a prior Poisson GLM, taking the anti-log of estimate for the lowest observed efficiency yields a decrease in U.S.-affecting hurricanes by a factor of 1.59 ($1 / e^{+0.009*-51.7}$); for the highest observed efficiency, an increase in frequency by a factor of 1.58 ($e^{+0.009*51.2}$).

Table 3.4 – Coefficients and Analysis of Deviance of a Poisson Regression Model for U.S.-affecting hurricanes (1851-2008) using SSN thermodynamic efficiencies (SSNε).

Term	Estimate	Degrees of Freedom	Deviance	Residual Degrees of Freedom	Residual Deviance	P-value
NULL	+0.575			157	196.42	
SSNε	+0.009	1	6.92	156	189.50	0.009

Figure 3.3 displays a histogram of SSN thermodynamic efficiencies for 1851 – 2008. Efficiencies are calculated by subtracting average peripheral-season month SSN (May, June, July, November) from average core-season month SSN(September). The distribution of SSN thermodynamic efficiencies produces a normal distribution (owing to the sinusoidal nature of annual SSN) with mean SSN efficiency -0.48 and a standard error of ± 17.09. Median SSN efficiency is +0.83. Almost 14 full solar cycles are represented in the dataset, comprising 2/3 of Solar Cycle 9 through all of Solar Cycle 23 (Kane 2002, 2009).

Next we examine hurricane seasons of highest and lowest SSN thermodynamic efficiencies. Seasons 1999, 1938, and 1929 are represented in Figure 3.4 (a, b, and c,

respectively). These years constitute the 3 highest calculated SSN thermodynamic efficiency seasons. The 1999 season (a) coincides with Solar Cycle 23 (Kane 2002, 2009 for all Solar Cycle number references), with the 2000 season displaying the cycle's peak (annual SSN
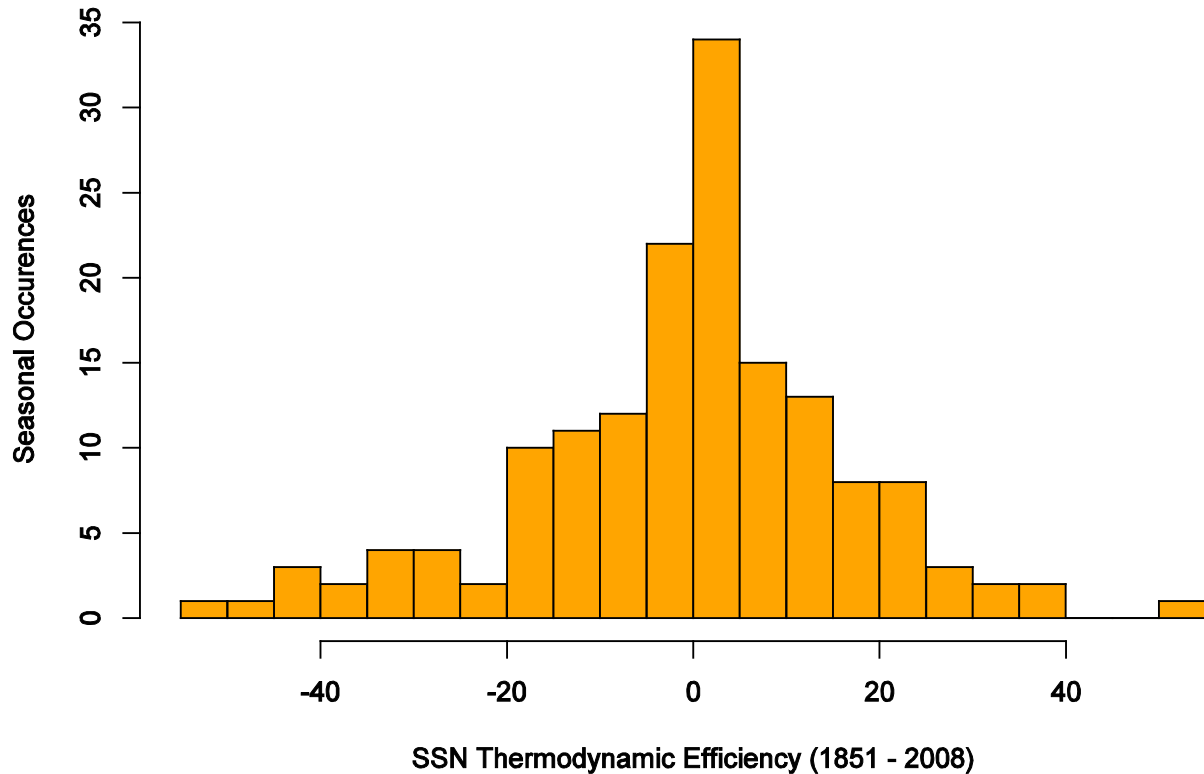
Figure 3.3 – Histogram of SSN thermodynamic efficiencies for 1851 – 2008. Individual efficiencies are calculated by subtracting average peripheral- season month SSN (May, June, July, and November) from core season month SSN (September).

average) as interpreted from its the subplot. The 1938 season (b) occurs within Solar Cycle 8, at or shortly-occurring after the cycle's peak. The 1929 season (c) occurs within Solar Cycle 7, just after the cycle's peak. In all 3 cases, elevated May, June, July, and November SSN coupled with lower September SSN led to the high efficiency calculation. Also of note is the period of occurrence within the solar cycle. On an annual time scale, efficiencies should theoretically be highest slightly after the cycle's peak due to decreasing solar activity. The 1938 and 1929 seasons fit within this line of thinking. However, the 1999 season occurred within a still-increasing solar cycle. Regardless, intrannual (monthly) SSN variation ultimately dominates the

24

Figure 3.4 – Monthly SSN (main plot) and surrounding annual SSN averages (subplot) for the highest SSN efficiency seasons of (a) 1999, (b) 1938, and (c) 1929.

thermodynamic calculation.

SSN for hurricane seasons 1978, 2001, and 1957 are represented in Figure 3.5 (a, b, and c, respectively). These years constitute the 3 lowest calculated SSN thermodynamic efficiency seasons. The 1978 season (a) occurs within Solar Cycle 21, just prior to the SSN cycle peak of the 1979 season. The 2001 season (b) occurs within Solar Cycle 23, just after the SSN cycle peak season of 2000. The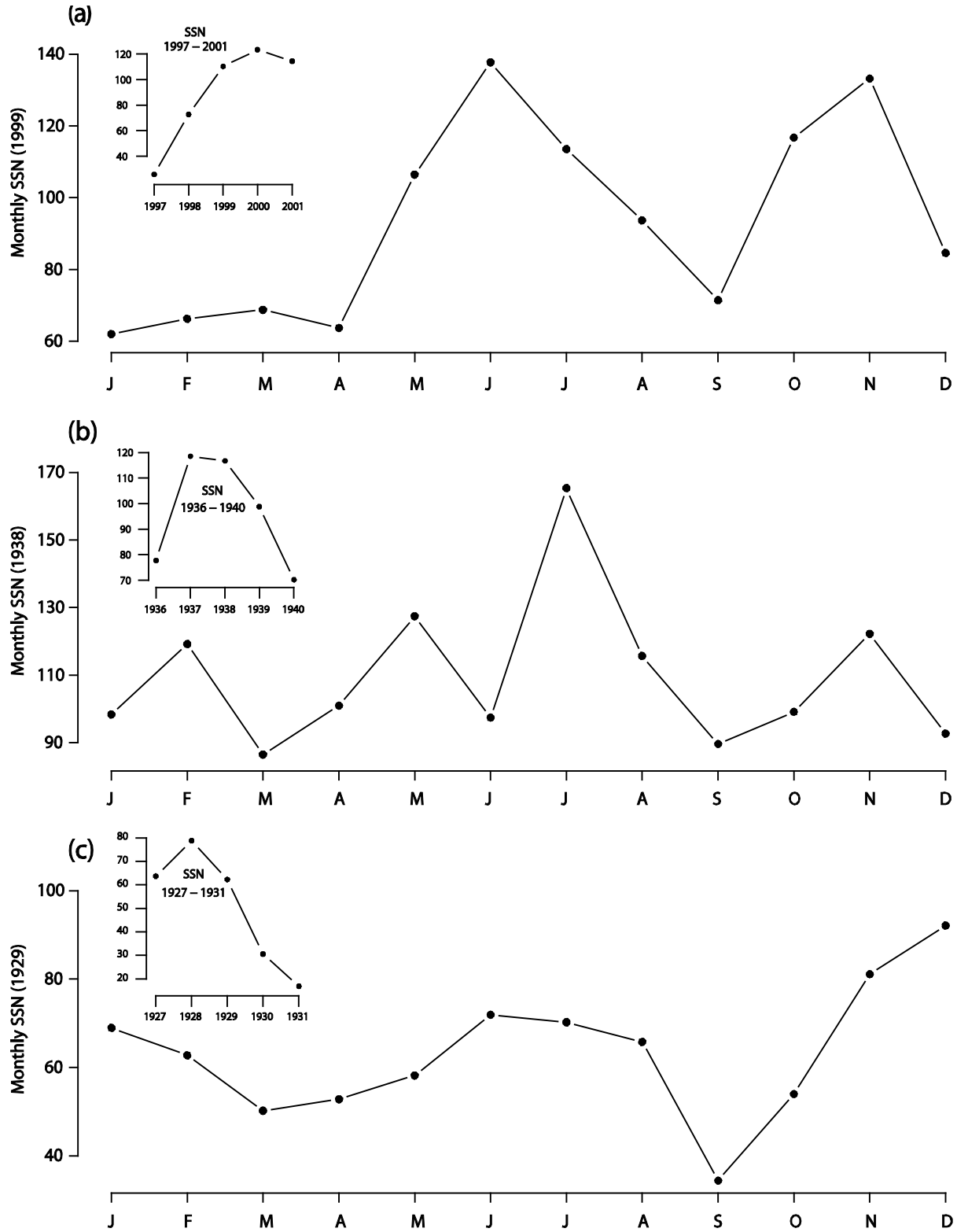 1957 season (c) occurs within Solar Cycle 19, the SSN cycle peak. All 3 cases demonstrate the opposite process displayed in the highest efficiencies: Lower May, June, July, and November SSN coupled with high September SSN resulting in low efficiencies. Ignoring Intraseasonal (monthly) variation, seasonal efficiencies should theoretically be highest slightly before cycle peaks due to increasing solar activity. Only the 1978 season agreed with this line of thinking. As with the low efficiency seasons, monthly SSN variation ultimately dominates the thermodynamic calculation.

Table 3.5 – Highest (left) and lowest (right) SSN thermodynamic efficiencies (SSNε) for 1851 – 2008. Mean SSNε, seasonal (monthly-averaged) SSN (Mean SSN), U.S.-affecting hurricane counts (U.S.), and major U.S.-affecting hurricane counts (> Category 3 on Saffir-Simpson scale) are also listed.

Year	SSNε	Mean SSN	U.S.	Major U.S.		Year	SSNε	Mean SSN	U.S.	Major U.S.
1999	+51.2	110.4	3	1		1978	- 51.7	95.4	0	0
1938	+38.5	116.7	2	1		2001	- 46.0	114.5	0	0
1929	+36.0	62.2	3	1		1957	- 45.0	201.6	1	1
1950	+32.6	76.2	3	2		1908	- 43.4	54.8	1	0
1871	+31.1	103.6	3	1		1981	- 42.4	141.2	0	0
1937	*+37.9*	*+93.8*	*2.8*	*1.2*		*1965*	*- 45.7*	*121.5*	*0.4*	*0.2*

Continuing the investigation, Table 3.5 represents the top 5 positive and negative SSN thermodynamic efficiency seasons, along with seasonal averages and total U.S.-affecting hurricane counts within the modern dataset. 14 total (2.8 / season) U.S.-affecting hurricanes were observed during the 5 highest efficiency seasons. 2 total (0.4 / season) U.S.-affecting hurricanes were observed during the 5 lowest efficiency seasons. Difference in mean rates is 2.4 U.S.-affecting hurricanes. 6 total (1.2 /season) major hurricanes (> Category 3) affected the U.S during the highest efficiency seasons, compared to 1 (0.2 / season) during low efficiency
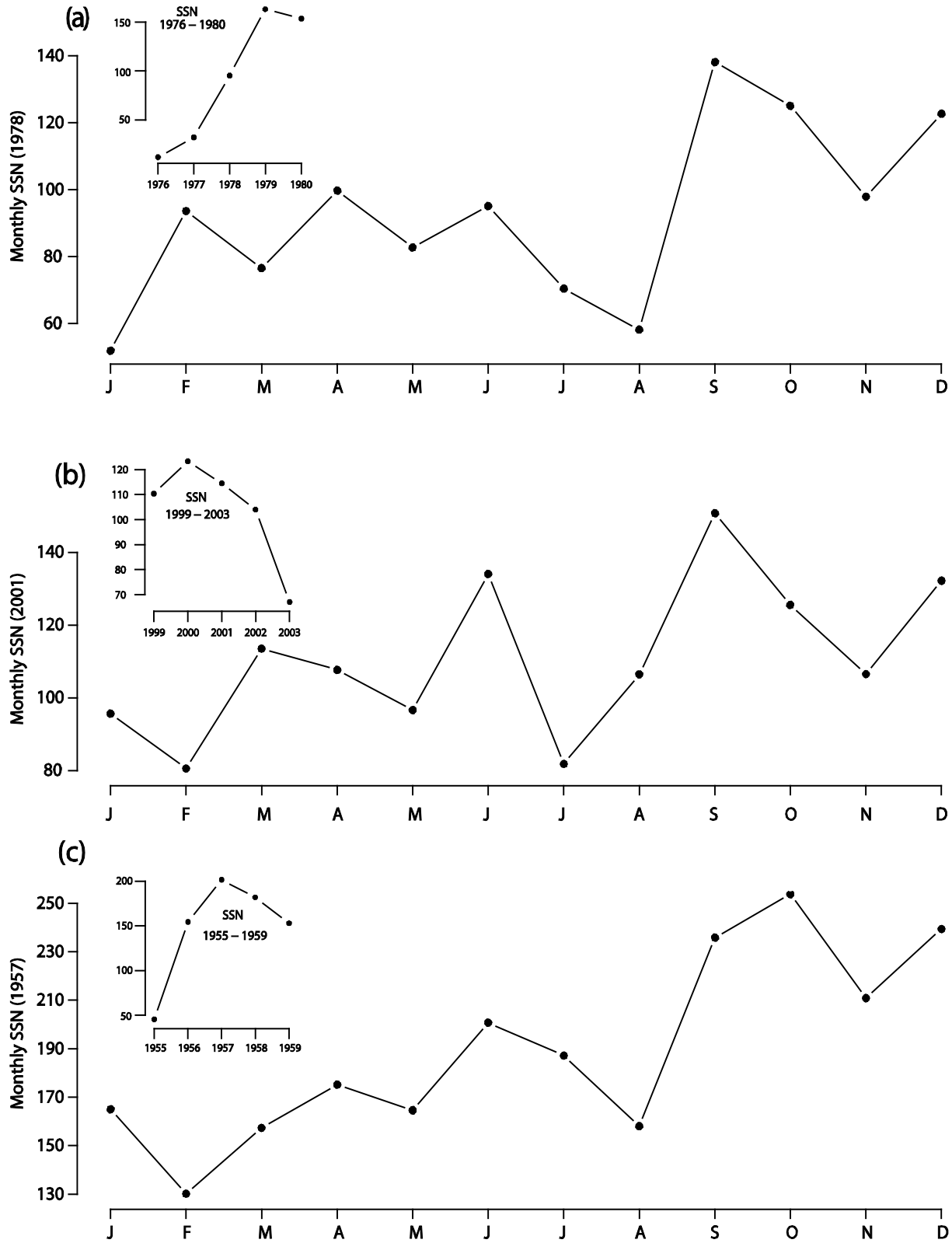
Figure 3.5 - Monthly SSN (main plot) and surrounding annual SSN averages (subplot) for the lowest SSN efficiency seasons of (a) 1978, (b) 2001, and (c) 1957.

seasons. Difference in mean seasonal rates is 1.0 U.S.-affecting major hurricanes.

The highest 5 efficiency seasons yielded 93.8 annually averaged SSN, while the lowest 5 efficiency seasons averaged 121.5 annually averaged SSN. The range of values indicates there is no significant relationship between mean annual SSN and SSN seasonal efficiency. While a weakly positive correlation coefficient exists between the two variables for the entirety of modern data (0.12), the finding is not statistically significant (P = 0.13). In this section we have discussed evidence for a solar influence upon U.S.-affecting hurricane frequency using modern records. Continuing the investigation started by Elsner & Jagger (2008) we examined SSN as a mitigating factor upon U.S.-affecting hurricanes for all available modern data. Increasing SSN data, conditioned on warm and cool SST anomaly phases, demonstrated a reduction in mean U.S.-landfalling hurricane frequency. SST above the 60th percentile yielded (statistically significant) increasing correlation coefficients between September SSN and U.S.-affecting hurricanes. Several seasonal models were constructed toward more accurately characterizing the sun-hurricane relationship, featuring permutations of such covariates as core-season SST and core-season SSN. Models were then used to explore intraseasonal SSN as covariates, with the construction of a thermodynamic efficiency (SSNε). In all cases, the model covariates significantly impacted the U.S.-affecting hurricane frequency toward supporting the thermodynamic link between warmed UTT and decreasing U.S.-affecting hurricanes. Ultimately, a model was constructed utilizing SSN as a sole-source (temporally partitioned) data source for investigating the sun-hurricane relationship. Highest and lowest efficiencies demonstrated marked associations with U.S.-affecting hurricane intensity and frequency consistent with the previous sun-hurricane findings.

The next section will continue with the SSN thermodynamic efficiency (hereafter, SSNε) as means for explicating the sun-hurricane relationship in light of newly available North Atlantic hurricane records. An additional 100 years of combined hurricane and SSN records (1749-1850) will be utilized to test whether or not the relationship corroborates findings in the modern records.

CHAPTER 4

EVIDENCE FOR A SOLAR INFLUENCE USING PRIOR RECORDS

SST anomaly data extends back only to 1856, disallowing joint SSN-SST / U.S. count regression prior. However, our discovery of a unique relationship between peripheral and core season SSN provides a method to extract information about U.S.-affecting hurricane activity using additional hurricane records (Chenoweth archive) and SSN.

Therefore, we will use available SSN and corroborating portions of the Chenoweth archive as means for describing the thermodynamic efficiency impact upon U.S.-affecting hurricane frequency in a Bayesian generalized linear model (GLM). Similar to the approach taken by Elsner & Bossak (2001), a Bayesian approach toward "a predictive climate distribution of coastal hurricane activity" can account for potentially problematic historical observations while providing meaningful results. We first examine the thermodynamic efficiencies calculated within the corroborating portions of the Chenoweth archive, 1749-1850.

SSN Thermodynamic Efficiencies

As described in Chapter 3, the SSN thermodynamic efficiency (SSNε) accounts for multicollinearity between the peripheral and core season month SSN while effectively

Table 4.1 – Highest (left) and lowest (right) SSN thermodynamic efficiencies (SSNε) for 1749 - 1850. Mean SSNε, seasonal (monthly-averaged) SSN, and associated U.S.-affecting hurricane counts (U.S.) are also listed.

Year	SSNε	Mean SSN	U.S.		Year	SSNε	Mean SSN	U.S.
1794	+40.3	41	2		1847	- 73.0	98.4	0
1837	+38.6	138.3	4		1839	- 67.2	85.7	1
1781	+34.7	68.1	2		1846	- 49.1	61.5	1
1838	+30.8	103.2	2		1835	- 41.7	56.9	4
1749	+29.6	80.9	1		1769	- 40.1	106.1	1
1800	*+34.8*	*86.3*	*2.2*		*1827*	*- 54.2*	*81.7*	*1.4*

representing the ambient storm seasonal environment. Figure 4.1 represents a histogram of SSN thermodynamic efficiencies for the 100 years of prior records. Mean SSNε is + 0.14 with a standard error of 18.64. The median SSNε is + 1.73. Only 9 solar cycles occurred during the 1749 – 1850 period, comprising all of Solar Cycle 1 and most of Solar Cycle 9 (Kane 2002, 2009). The two lowest efficiencies for the entirety of data (1749-2008) occur in the premodern records in 1847 (-73.0) and 1839 (-67.2), as evidenced from Table 5.1. Only 1 U.S.-affecting hurricane was recorded during this period. For the highest 5 SSNε seasons, 11 (2.2 / season) total U.S.-affecting hurricanes were recorded; for the lowest 5 SSNε seasons, 7 (1.4 / season) were recorded, resulting in a mean difference in rates of 0.8 hurricane per season. This result is less than the modern record SSNε comparison (2.4 / season), but marginally equivalent to the difference in mean seasonal rates for modern major U.S.-affecting hurricanes (1.0 / season). Given that major hurricanes (> Category 3 on the Saffir-Simpson scale) are more likely to be
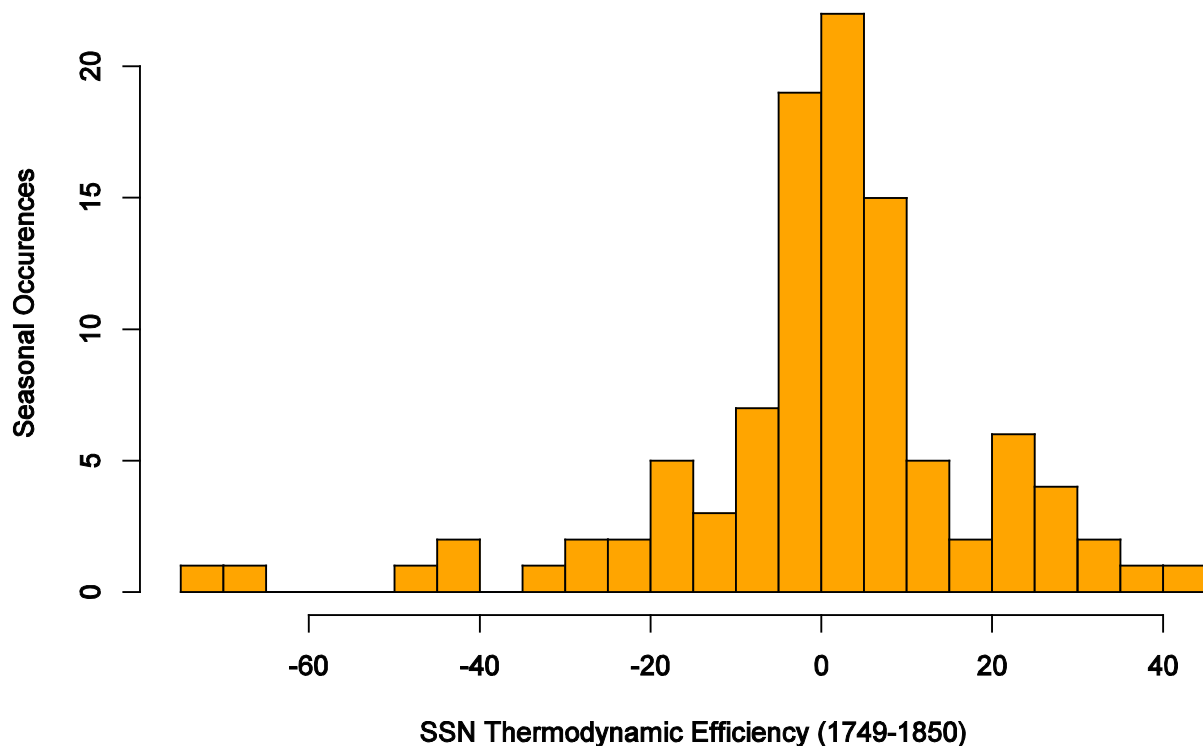

Figure 4.1 - Histogram of SSN thermodynamic efficiencies for 1749 –1850. Individual efficiencies are calculated by subtracting average peripheral season month SSN (May, June, July, and November) from core season month SSN (September).

recorded given their breadth of destructiveness (storm-surge and winds, primarily), the analogous rates between modern major U.S.-affecting hurricanes and prior record hurricanes could be demonstrating that the prior record hurricanes were, in fact, major hurricanes.

SSNε will constitute the lone covariate in the Bayesian GLMs. In the next section we will address statistical modeling techniques toward explicating the sun-hurricane relationship (SSNε) in light of prior hurricane records.

Modeling Approaches

Three models are generated utilizing SSNε. A Bayesian GLM In addition to a Bayesian model, an alternate Bayesian GLM is additionally constructed to identify the value and contribution of the Bayesian model. Each represents a methodological approach to tempestology regarding the use of storm observation records. For all models, SSNε data is scaled (subtracting the mean and dividing by the standard deviation) to produce standardized values. The scaled values facilitate calculation of the prior distribution model parameters for the Bayesian models.

The *Conservative* approach used here argues that the strength of explanatory statistics is commensurate to the quality of data being analyzed, with HURDAT providing storm-specific information back to 1851; as such, questionable data is no data at all. Therefore, the range of data is 1851-2008. The *Bayes* approach utilizes the 102 prior years of U.S.-affecting hurricane counts from Chenoweth (2006) as a source of information to further elucidate the relationship as currently understood in the modern data. The *Wrong_info Bayes* approach is identical to *Bayes*, except that prior hurricane counts and corresponding years are randomized, obscuring any potential storm count / SSN relationship in the prior distribution formation. The *Bayes* and *Wrong_info Bayes* both represent posterior distributions.

Bayesian Approach

The Bayesian method represents a statistical approach that incorporates additional information, referred to as the prior distribution, as a random variable "to update an initial state of knowledge to a new state of knowledge," producing the posterior distribution (O'Hagan

2006). In our case, the prior distribution is 102 years of additional U.S.-affecting hurricane counts and SSN data, elicited from a Poisson GLM of SSNε for 1749-1850. The posterior distribution utilizes prior distribution information toward a multiple-permutation Bayesian GLM of U.S.-affecting hurricane counts regressed upon SSNε. The construction of the prior distribution will be expanded upon later.

Before proceeding, we acknowledge a limitation of the historical data set. Figure 4.2 represents a histogram of U.S.-affecting hurricane counts, bifurcated by the Chenoweth archive and HURDAT periods. Time-count autocorrelation is negative yet not significant (slope = -0.001, P = 0.575) within the modern record, but is positive and significant (slope = +0.006, P = 0.042) within the 1749-1850 portion of the Chenoweth (2006) archive.
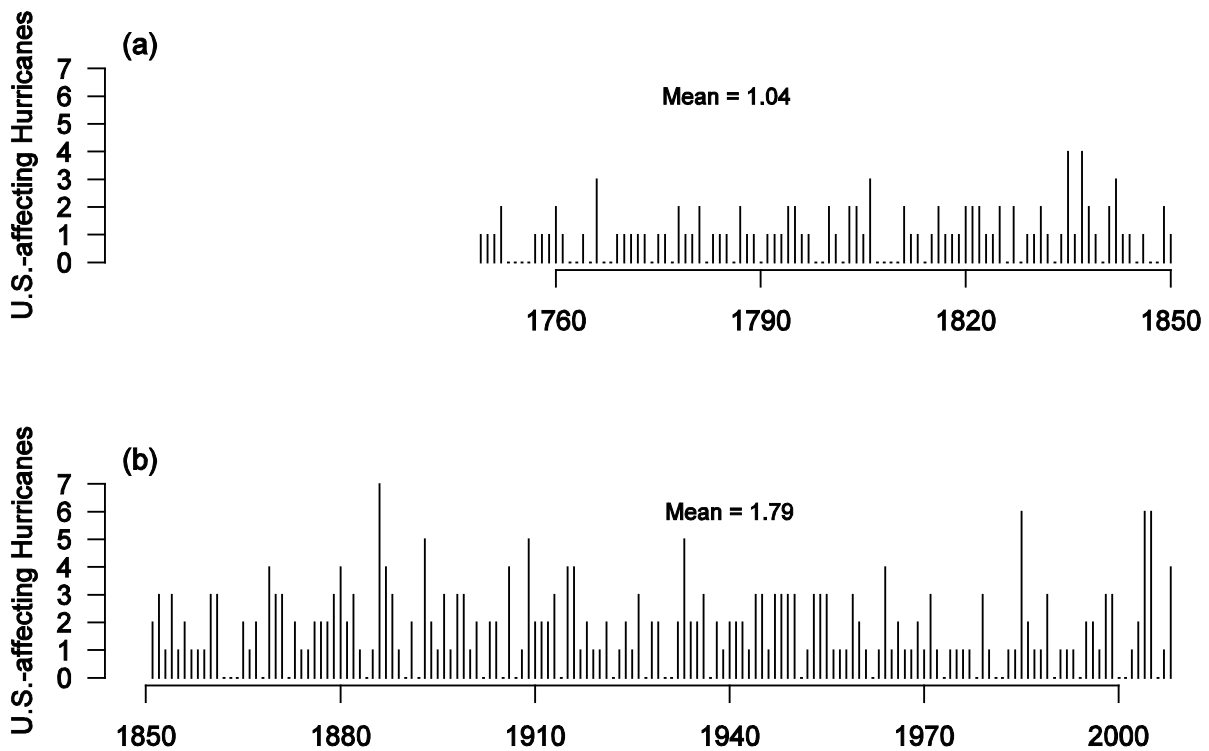
Figure 4.2 – U.S.-affecting hurricane counts for the periods (a) 1749-1850 (Chenoweth archive) and (b) 1851-2008 (HURDAT).

To appropriately incorporate the portion of the Chenoweth archive toward a posterior understanding of thermodynamic efficiency and U.S. counts, we statistically address the time-

Table 4.2 – Population totals for the Caribbean (Engerman 2000) and geographic U.S. (Abstract 1997).

Year	Caribbean	U.S.	Combined
1700	310,000	250,900	560,900
1750	1,000,000	1,170,800	2,170,800
1800	2,200,000	5,308,483	7,508,483
1850	4,000,000	23,191,876	27,191,876

Figure 4.3 – Process for accounting for time-correlation within 1749-1850 portion of the Chenoweth archive: (a) observed storm counts, (b) missing storm rate, (c) a single simulation of seasonal missed storms, and (d) simulated plus observed storm counts. Missing storm rates (b) are only calculated up through 1850.

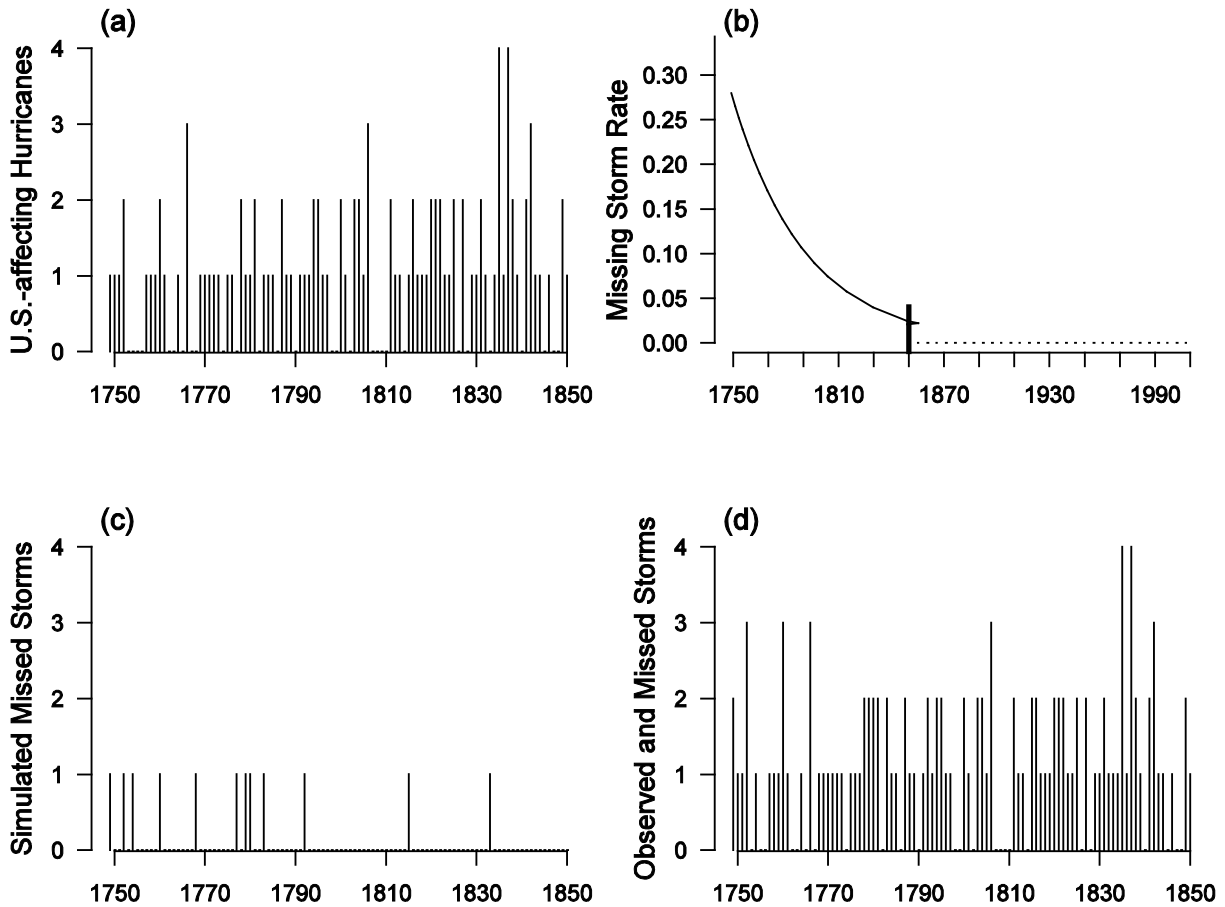opportunity for observation is a limiting factor toward U.S.-affecting hurricane information compilation. Table 4.2 lists U.S. and Caribbean population totals since 1700. Using the time series of population totals, we infer from the combined populations an exponential relationship of growth that will serve as a metric of our "opportunity for observation." The negative of the observed rate is taken for use toward calculating a missed rate of observed storms, yielding

$$Y = e^{(-0.026*(YY-1700))}$$

where YY represents the storm year from 1700 to 1850.

A sample of missed storms (Figure 4.3c) are randomly generated (Poisson) for the duration of the included Chenoweth archive storms based on the missed rate of observed storms (Figure 4.3b). The sample is then added back to the original observation time series, creating a combination of observed and probable missed storm counts (Figure 4.3d). This missing rate serves as the dependent variable within a standard GLM against SSNε as covariate 1749-1850. Since the missing storm rate is used in a Poisson random generation, the process is repeated 1,000 times to account for aleatory uncertainty produced from the sampling process. The resulting parameter and variance model estimates are recorded and serve as our prior information toward determining a posterior distribution of SSNε.

Model Results

The P-value is computed by determining the count of simulations resulting in an estimate less than zero, and then dividing this number by the number of simulations. 100,000 permutations are conducted for each model. Parameter estimates and associated P-values are listed in Table 4.3. Model parameter estimates and variances for the SSNε – U.S.-affecting hurricane frequency in each model vary for each run of the model, producing varying coefficients per permutation. Statistical modeling represents this uncertainty with a standard error. Figure 4.4 is a density plot of the 100,000 accumulated parameter estimates for each model run. The sum of the parameter estimates divided by the total permutations (100,000) is the mathematical representation of the regression parameter estimate for the model represented in Table 4.3. The standard error is
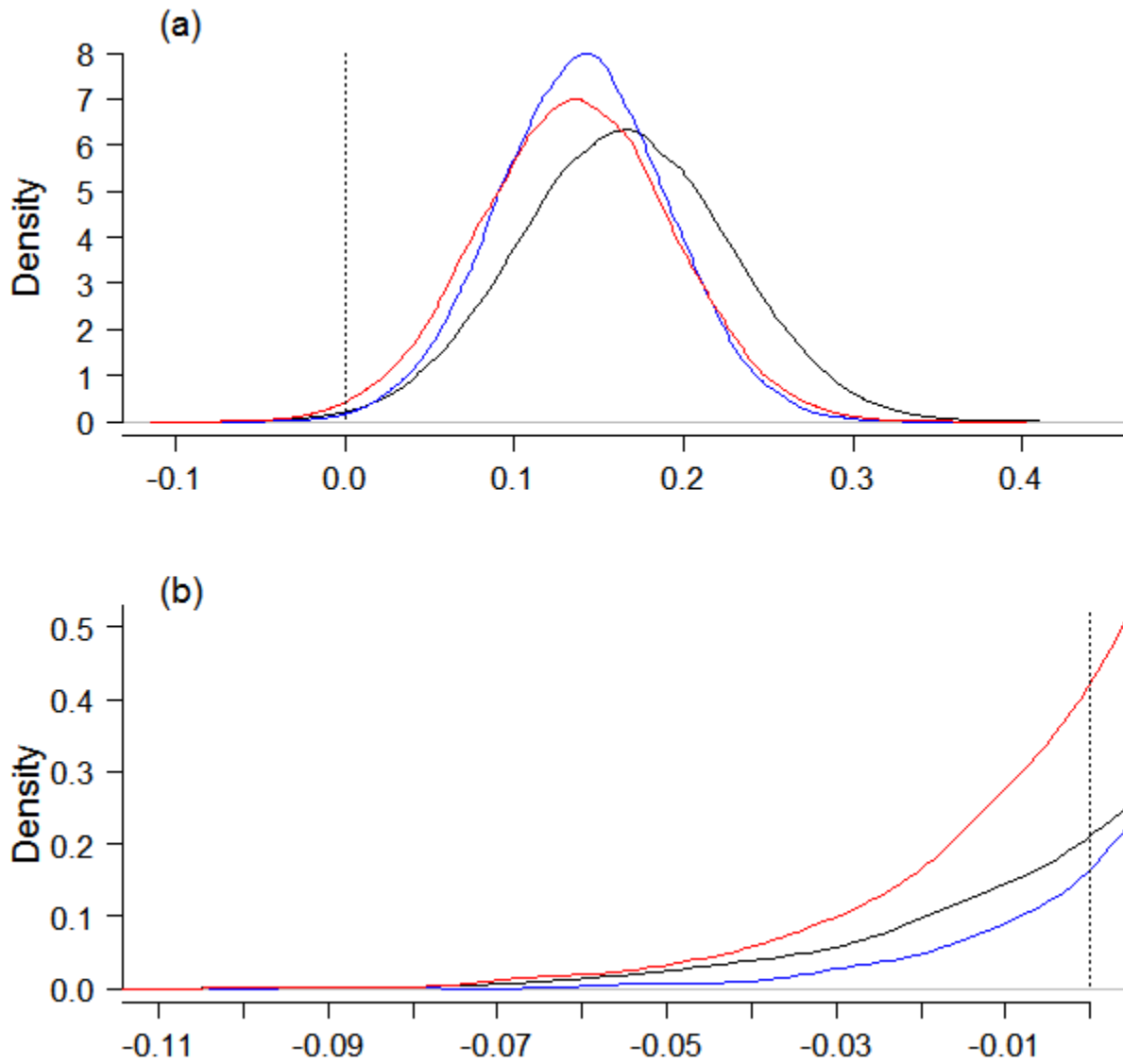
Figure 4.4 – Density estimates for *Conservative* (black), *Bayes* (blue), and *Wrong_info Bayes* (red) model parameter estimates. The area under each line to the left of 0 represents each model P-value.

Table 4.3 – Coefficients and P-values from Bayesian Poisson Simulated Regression Models

Model	Estimate	P-value
Conservative	+ 0.165	0.009
Bayes	+ 0.140	0.006
Bayes (Wrong_info)	+ 0.136	0.017

realized in Figure 4.4 as represented by the dispersion of the parameter estimates for each model. Model P-values are calculated as the area under the parameter estimate density to the left of 0.

The greatest magnitude of parameter estimates is found within the *Conservative* model. The strongest p-value coincides with the *Bayes* model. The *Wrong_info Bayes* model produced the smallest parameter estimate and P-value out of all 3 models, which is expected. "Wrong information" should degrade the quality of the posterior distribution. The SSNε – U.S.-affecting hurricane frequency relationship was found to be significant in all 3 models.

The *Bayes* model reveals a positive estimate (+0.140) at strong statistical significance (P = .006). The positive estimate is based on scaled data as described earlier in this section, but the sign of the coefficient (and statistical significance) mirrors the findings of the modern record SSNε – U.S.-affecting hurricane frequency results from Chapter 3.

The *Bayes* and *Wrong_info Bayes* model yield similar yet interestingly different results. With randomized annual storm counts serving as used toward generating the prior distribution, the *Wrong_info Bayes* model produced a less concise distribution compared to the *Bayes* model. This is significant; the increase in parameter estimate magnitude and conciseness of distribution indicates that the prior source of hurricane counts and associated SSN information supports the relationship found within the modern record.

Summary & Future Work

The goal of this study was to test the robustness of the hypothesis that the sun modulates U.S. hurricane activity. The relationship is described by an inverse correlation between the probability of a U.S. hurricane and the number of sunspots. It is speculated that increased solar activity increases UV radiation absorption by ozone and, thusly, inhibits hurricane intensity based on the maximum potential intensity argument that the magnitude of difference between inflow and outflow temperatures constitutes a thermodynamic efficiency in converting heat into wind.

Temporally segmenting the modern data by analyzing solar activity during the climatological peak (September) of the North Atlantic hurricane season provides an initial if not statistically significant foray into elucidating further information about the sun-hurricane relationship. After incorporating another significant hurricane intensity variable (SST) as an

additional partitioning into the relationship, the mean number of U.S.-affecting hurricanes decreases by 20% for cooler season SST / higher September SSN (as compared to lowest September SSN). Seasons of comparatively warmer SST yielded higher magnitude (negative) correlation coefficients between September SSN and U.S.-affecting storm counts. A Poisson regression model is used to corroborate these findings.

One of the primary contributions of this work is the creation of a temporal thermodynamic efficiency for SSN, where core and peripheral month SSN constitute an efficiency index to MPI in terms of inflow (SST) and outflow (UTT) temperatures. The modeled parameter estimate of this efficiency upon storm count yielded a significant negative coefficient, suggesting a suppression of hurricane development due to warmer September UTT and/or cooler seasonal SST consistent with a minimal energy efficiency scenario within the MPI theoretical framework.

With the Elsner & Jagger (2008) spatial contribution and this study's temporal explication of modern data supporting a segmenting of SSN toward an impact upon U.S.-affecting hurricane counts, the sun-hurricane relationship's robustness is tested in light of historic hurricane information. Using this information meaningfully, a Bayesian approach is justified and compared with other methodological approaches to simulated model results. Utilizing the information contained within the Chenoweth archive, the results add measurable support to the hypothesis that solar variation influences hurricane activity.

Future work may include other UV indices, such as the Mg II index used in Hood (2003), along with theoretical thermodynamic calculations to look at storm velocities in modern data. Whereas this study examined an intraseasonal thermodynamic proxy, such information could be studied daily. Also, as prior hurricane records improve due to improved historical recovery, the SSNε – U.S.-affecting hurricane frequency relationship may yield even more significant results. On a longer time scale, future work to push the boundaries of hurricane records would provide a fascinating study coinciding with a major solar cycle minimum event, the Maunder minimum. This period featured a global temperature reduction and minimal sunspots (Vaquero et al. 2002). With some scientists predicting lower amplitude solar cycles (Duhau 2003; Dikpati et al. 2006; Rai 2007), an analog such as the Maunder minimum study could provide further insight into the sun-hurricane relationship.

REFERENCES

Ackerman, S. A., & J. A. Knox (2003): <u>Meteorology: Understanding the Atmosphere.</u>
Brooks/Cole, 486 pp.

American Meteorological Society (2009): AMS Glossary: C. Glossary of Meteorology. Allen
Press, Retrieved on 2009-3-15, Web site:
http://amsglossary.allenpress.com/glossary/browse?s=c&p=19.

Aerosonde (2006): Aerosonde first UAV to penetrate a Tropical Cyclone. Retrieved on 2008-12-
09, Web site: http://www.aersonde.com/drawarticle/127

Allison, P.D. (1999): <u>Multiple regression: A primer</u>. Thousand Oaks, Calif. Pine Forge Press,
202 pp.

Anthes, R. A. (1982): <u>Tropical cyclones – Their evolution, structure, and effects</u>. Monograph No.
41, American Meteorological Society, 208 pp.

ASOS User's Guide – National Weather Service (1998): Executive Summary. Retrieved on
2008-03-01, Web site: http://www.weather.gov/asos/pdfs/aum-toc.pdf

Assembly of Mathematical and Physical Sciences (U.S.). Geophysics Study Committee (1997):
The upper atmosphere and magnetosphere. National Academy of Sciences.

Atlantic Oceanic and Meteorological Laboratory - National Oceanic and Atmospheric
Administration (2008): HURDAT Re-analysis. Retrieved on 2008-03-21, Web site:
http://www.aoml.noaa.gov/hrd/hurdat/.

Basu, S.. & H.M. Antia (2008): Helioseismology and Solar Abundances. *Physics Reports,* **457**
(217), doi:10.1016/j.physrep.2007.12.002.

Bister M., & K. A. Emanuel (1998): Dissipative heating and hurricane intensity. *Meteor. Atmos.
Phys*, **50**, pp. 233–240.

Bogen, K. T., E. D. Jones & L. E. Fischer (2007): Hurricane destructive power predictions based
on historical storm and sea surface temperature data. *Risk Analysis,* **27,** pp. 1497-1517.

Brasseur, G., & S. Solomon (2005): <u>Aeronomy of the middle atmosphere: Chemistry and physics
of the stratosphere and mesosphere.</u> 3rd ed., Springer Publishing, 644 pp.

Earth System Research Laboratory: Physical Sciences Division (2009): ESRL : PSD : Download
Climate Timeseries: AMO SST. Retrieved January 1, 2009, Web site:
http://www.cdc.noaa.gov/data/timeseries/AMO/

Chenoweth, M. (2006): A reassessment of historical Atlantic basin tropical cyclone activity,
1700-1855. *Climatic Change,* **76,** pp. 169-240.

Dikpati, M., G. de Toma, & P. A. Gilman (2006): Predicting the strength of solar cycle 24 using a flux-transport dynamo-based tool. *Geophys. Res. Lett*., **33**, pp. L05102.

Dong K., & C. J. Neumann (1986): The relationship between tropical cyclone motion and environmental geostrophic flows. *Mon. Wea. Rev*., **114**, pp. 115–122.

Duhau, S. (2003): An Early Prediction of Maximum Sunspot Number in Solar Cycle 24. *Solar Physics*, **213**(1), pp. 203-212.

Elsner, J. B. & B. H. Bossak (2001): Bayesian analysis of US hurricane climate. *J. Clim.,* **14,** pp. 4341-4350.

Elsner, J. B. & A. B. Kara (1999): Hurricanes of the North Atlantic: Climate and society. Oxford: Oxford University Press, 488 pp.

Elsner, J. B., & T. H. Jagger (2008): United States and Caribbean tropical cyclone activity related to the solar cycle. *Geophys. Res. Lett.*, **35**, pp. L18705, doi:10.1029/2008GL034431.

Elsner, J.B., J.P. Kossin, & T.H. Jagger (2008): The increasing intensity of the strongest tropical cyclones. *Nature*, **455**, pp. 92-95.

Elsner, J. B., T. H. Jagger, & K. B. Liu (2008): Comparison of hurricane return levels using historical and geological records. *Journal of Applied Meteorology and Climatology,* **47,** pp. 368-374.

Emanuel, K. A. (1991): The theory of hurricanes. *Annu. Rev. Fluid. Mech.*, **23**, pp. 179– 196.

Enfield, D.B., A.M. Mestas-Nunez, & P.J. Trimble (2001): The Atlantic Multidecadal Oscillation and its relationship to rainfall and river flows in the continental U.S. *Geophys. Res. Lett.*, **28**, pp. 2077-2080.

Engerman, S.L. (2000): A Population History of the Caribbean. In M. Haines & R. Steckel (Ed.), A population history of North America (pp. 483-528), Cambridge University Press.

Fermi, E. (1956): Thermodynamics. Courier Dover Publications, 160 pp.

Fernandez-, J. & Diaz, H. F. (1996): *A Reconstruction of Historical Tropical Cyclone Frequency in the Atlantic from Documentary and Other Historical Sources, Part III: 1881–1890.* Climate Diagnostics Center, Environmental Research Laboratories, National Oceanic and Atmospheric Administration, Boulder, CO., available at http://www.aoml.noaa.gov/hrd/hurdat/hurdat pub.html

Ghosh, S N. (2002): The neutral upper atmosphere. Kluwer Academic Publishers, 205 pp.

Gray, W. M. (1968): Global view of the origin of tropical disturbances and storms. *Mon. Wea. Rev.,* **96,** pp. 669–700.

Heath, D., & B. Schlesinger (1986): The Mg 280 nm doublet as a monitor for changes in solar ultraviolet irradiance. *J. Geophys. Res*., **91**, pp. 8672-8688.

Henderson-Sellers, A., H. Zhang, G. Berz, K. Emanuel, W. Gray, C. Landsea, G. Holland, J. Lighthill, S.L. Shieh, P. Webster, & K. McGuffie (1998): Tropical Cyclones and Global Climate Change: A Post-IPCC Assessment. *Bull. Amer. Meteor. Soc.*, **79**, pp. 19–38.

Holland, G. (1997): The maximum potential intensity of tropical cyclones. *J. Atmos. Sci.*, **54** (21), pp. 2519-2541.

Hood, L.L. (2003): Thermal response of the tropical tropopause region to solar ultraviolet variations. *J. Geophys. Res*., **30**(23), pp. 2215(10/1-4), doi:10.1029/2003GL018364

Hoyt, D. V., & K. H. Schatten (1997): The Role of the Sun in Climate Change. Oxford, 279 pp.

Hurricane Research Team (2006): Texas Tech Hurricane Research Team Project History and Information - Texas Tech University. Retrieved on 2006-03-30, Web site: http://www.atmo.ttu.edu/WEMITE/introduction.htm

Incropera, F.P, & D.P. De Witt (1996): Fundamentals of Heat and Mass Transfer. 4th ed., John Wiley & Sons, 886 pp.

Jarvinen, B., C. Neumann, & M. Davis (1984): *A tropical cyclone data tape for the North Atlantic Basin, 1886-1983: Contents, limitations, and uses*. NOAA Tech. Memo, NWS NHC-22, pp. 21, National Oceanic & Atmospheric Administration, Washington, D.C.

Labitzke, K. (2002): The global signal of the 11-year solar cycle in the stratosphere: observations and models. *Journal of atmospheric and solar-terrestrial physics*, **64**(2), pp. 203-210.

Kane, R.P. (2002): Some Implications Using the Group Sunspot Number Reconstruction. *Solar Physics*, **205**(2), pp. 383-401.

--- (2009): Fluctuations of Solar Activity during the Declining Phase of the 11-Year Sunspot Cycle. *Solar Physics*, **255**(1), pp. 163-168.

LaRow, T.E., Y.K. Lim, D.W. Shin, E.P. Chassignet, & S. Cocke (2008): Atlantic Basin Seasonal Hurricane Simulations. *J. Clim.*, **21**, pp. 3191–3206.

van Loon, H., & D.J. Shea (1999): A probable signal of the 11-year solar cycle in the troposphere of the northern hemisphere. *J. Geophys. Res*., **26**, pp. 2893–2896.

Ludlum, D. (1963): Early American Hurricanes: 1492-1870. American Meteorological Society, Boston, Mass., 198 pp.

Mann, M. E., & K. A. Emanuel (2006): Atlantic Hurricane Trends Linked to Climate Change. *Eos Trans. AGU*, **87**(24), doi:10.1029/2006EO240001, pp. 233-244.

Meldrum, C. (1872): On a periodicity in the frequency of cyclones in the Indian Ocean south of the equator. *Nature*, **6**, pp. 357-358.

Miller, B. I. (1958): On the maximum intensity of hurricanes. *J. Meteor.*, **15**, pp. 184–195.

National Hurricane Center (2008): National Weather Service, National Hurricane Center. Retrieved 21-01-2009. Web site: http://www.nhc.noaa.gov/tracks1851to2007_atl_reanal.txt.

O'Hagan, A., C.E. Buck, A. Daneshkhah, J.R. Eiser, P.H. Garthwaite, D.J. Jenkinson, J.E. Oakley, & T. Rakow (2006): Uncertain Judgements: Eliciting Experts' Probabilities. John Wiley & Sons, 338 pp.

Palmen, E. H. (1948): On the formation and structure of tropical cyclones. *Geophysica,* **3,** pp. 26–38.

Pap, J.M., & P. Fox (2004): Solar Variability and its Effects on Climate. AGU Press, 366 pp.

Poey, A. (1855): A chronological table comprising 400 cyclone hurricanes which have occurred in the West Indies and in the North Atlantic within 362 years, from 1493-1855. *J. Royal Geog. Soc., 25*, pp. 291-328.

--- (1873): Sur les rapports entre les taches solaires et les ourages des Antilles de l'Atlantique-nord et de l'Ocean Indien sud. *Compt. Rend.*, **77**, pp. 1223–1226.

R Development Core Team (2006): R: A language and environment for statistical computing and graphics. R Found. for Stat. Comput., Vienna, Austria. (Available at http://www.R-project.org)

Rai, C.A., C. Piyali, & J. Jie (2007): Predicting solar cycle 24 with a solar dynamo model. *Physical review letters*, **98**(13), pp. 131103.

Redfield, W.C. (1836): On Gales and Hurricanes of the Western Atlantic. *U.S. Naval Magazine*, **1,** and *London Nautical Magazine*, **5**.

Rybicki, G. B., & A.P. Lightman (1979): Radiative Processes in Astrophysics. John Wiley & Sons, 400 pp.

Salpeter, E.E. (1952): Nuclear Reactions in the Stars. I. Proton-Proton Chain. *Phys. Rev.*, **88**, pp. 547-553.

Scheitlin, K., J. Malmstadt, R. Hodges, J. Elsner, & T. Jagger (2009): Towards increased utilization of historic hurricane chronologies. *J. Geophys. Res.*, (in review).

Scott, P. (2006): <u>Hemingway's Hurricane: The Great Florida Keys Storm of 1935</u>. McGraw-Hill, 288 pp.

Smiley, C.H. (1959): Poisson's Law and the Frequency of Hurricanes. *Nature*, **183**, pp. 814-815, doi:10.1038/183814a0.

Stanford Solar Center (2009): Glossary. Retrieved on 2009-03-15, Web site: http://solar-center.stanford.edu/gloss.html

Statistical Abstract of the United States (1997): Historical Statistics of the United States: Colonial Times to 1970 - Bicentennial edition. 117th ed. Washington: Government Printing Office.

National Geophysical Data Center - National Oceanic and Atmospheric Administration (2009): Tables of Monthly Sunspot Numbers. Retrieved 12-01-2008,Web site: ftp://ftp.ngdc.noaa.gov/STP/SOLAR_DATA/SUNSPOT_NUMBERS/MONTHLY.

Van der Linden, R.A.M., & the SIDC team (2009): Online catalogue of the sunspot index. Retrieved on 02-01-2009, Web site: http://sidc.oma.be/html/sunspot.html

Vaquero, J.M., F. Sánchez-bajo, & M.C. Gallego (2002): A Measure of the Solar Rotation During the Maunder Minimum. *Solar Physics*, **207**(2), pp. 219.

Viereck, R., & L. Puga (1999): The NOAA Mg II core-to-wing solar index: Construction of a 20-year time series of chromospheric variability from multiple satellites, *J. Geophys. Res.*, **104**, pp. 9995-10005.

Weiss, N.O. (2007): Sunspot structure and dynamics. In D.N. Baker (Ed.) <u>Solar Dynamics and Its Effects on the Heliosphere and Earth</u>. Springer, pp. 13-22.

White, W.B., Lean, J., Cayan, D.R., Dettinger, M.D. (1997): Response of global upper ocean temperature to changing solar irradiance. *J. Geo. Res.*, **102**, pp. 3255–3266.

White, W.B., Cayan, D.R., Lean, J. (1998): Global upper ocean heat storage response to radiative forcng from changing solar irradiance and increasing greenhouse gas/aerosol concentrations. *J. Geo. Res.*, **103**, pp. 21355–21366.

BIOGRAPHICAL SKETCH

Date and Place of Birth

11 December 1981

Newport News, Virginia

Education

B.S., Meteorology. Florida State University, Tallahassee, FL, Spring 2004

M.S., Geography. Florida State University, Tallahassee, FL, Summer 2009

Relevant Experience

Research Assistant, Florida State University – Fall 2007- Summer 2009

Publications

Scheitlin, K., J. Malmstadt, R. Hodges, J. Elsner, and T. Jagger. (2009). Towards increased utilization of historic hurricane chronologies. J. Geophys. Res., (in review).

Presentations

Hodges,R.E., J.B. Elsner, & T.H. Jagger (2009) Evidence for a Solar Influence on U.S.-affecting Hurricanes. *2nd Annual International Summit on Hurricanes and Climate Change*. Corfu, Greece.